RSC Advances

REVIEW

View Article Online
View Journal | View Issue

Check for updates

Cite this: *RSC Adv.*, 2024, **14**, 31921

A review of the electrochemical and galvanic corrosion behavior of important intermetallic compounds in the context of aluminum alloys†

Alexander I. Ikeuba, *[aj] Chigoziri N. Njoku, [bjk] Okpo O. Ekerenam,[cj] Demian I. Njoku,[djkl] Inime I. Udoh, *[ej] Enobong F. Daniel, [fj] Paul C. Uzoma, *[gjm] Ini-Ibehe N. Etim *[hjkn] and Bright O. Okonkwo*[ij]

Received 21st August 2024
Accepted 26th September 2024

DOI: 10.1039/d4ra06070a

rsc.li/rsc-advances

Aluminum alloys are widely sought for different applications due to their high strength-to-weight ratio. Most often this increased strength of the alloy is achieved by specific alloying elements and heat treatment processes which give rise to second phases intermetallic particles (IMPs) also known as intermetallic compounds (IMCs). These second phases play a dominant role in the corrosion susceptibility of aluminum alloys. This review provides a systematic survey of the electrochemical, and galvanic corrosion behavior of IMPs in the context of aluminum alloys. A discussion of the electrochemical/galvanic corrosion behavior of selected/important intermetallic compounds that are commonly found in aluminum alloys such as the Q-phase ($Al_4Cu_2Mg_7Si_8$), π-phase ($Al_8Mg_3FeSi_6$), θ-phase (Al_2Cu), S-phase (Al_2CuMg), the β-phase (Mg_2Si), β-phase (Al_3Mg_2), δ (Al_3Li), η-phase ($MgZn_2$), and β-phase (Al_3Fe) is provided. In addition, the limitations in the electrochemical characterization of intermetallic compounds, the research gap, and prospects are also provided in addition to the phenomenon of galvanic polarity reversal and self-dissolution of IMPs.

Open Access Article. Published on 09 October 2024. Downloaded on 7/19/2025 2:17:10 AM.
This article is licensed under a Creative Commons Attribution-NonCommercial 3.0 Unported Licence.

1 Introduction

Despite corrosion problems faced by aluminum alloys, they are still extensively utilized in technical applications in the automotive, marine, and aerospace sectors.[1–4] The corrosion vulnerability of aluminum-based alloys is primarily linked to the inhomogeneous microstructural features (such as intermetallic phases) which depend on the alloying elements present. Intermetallic phases (also called intermetallic compounds or particles) are chemical compounds made up of two or more metals which occur in the microstructure of alloys with a stoichiometry different from that of the parent alloy. Different intermetallic compounds can lead to serious localized corrosion impairment.[5–8] This localized corrosion manifests more often as intergranular or pitting corrosion depending on whether the intermetallic compounds are dispersed or concentrated along the alloy matrix's grain boundary. The smaller the intermetallic compound, the lower the impact it has on the alloy when considering the localized corrosion. The electrochemical characteristics assigned to intermetallic compounds are often distinct from one another and the matrix of the aluminum alloy since they are compositionally different. The open circuit potential of an intermetallic substance is usually

[a]*Materials Chemistry Research Group, Department of Pure and Applied Chemistry, University of Calabar, Calabar, Nigeria. E-mail: ikeubaalexander@unical.edu.ng*
[b]*Environmental, Composite and Optimization Research Group, Department of Chemical Engineering, Federal University of Technology, PMB 1526, Owerri, Nigeria*
[c]*Department of Biochemistry, School of Pure & Applied Sciences, Federal University of Technology, Ikot Abasi, Akwa Ibom State, Nigeria*
[d]*Department of Applied Science, School of Science and Technology, Hong Kong Metropolitan University, Hong Kong SAR, China*
[e]*The Hempel Foundation Coatings Science and Technology Centre (CoaST), Department of Chemical and Biochemical Engineering, Technical University of Denmark (DTU), 2800 Kgs. Lyngby, Denmark. E-mail: inudoh@kt.dtu.dk*
[f]*Shenyang National Laboratory for Materials Science, Institute of Metal Research, Chinese Academy of Sciences, Shenyang 110016, China*
[g]*ZJU-UIUC Institute, Zhejiang University, International Campus, Haining 314400, China. E-mail: pauluzoma@futo.edu.ng*
[h]*Marine Chemistry and Corrosion Research Group, Department of Marine Science, Akwa Ibom State University, PMB 1167, Nigeria. E-mail: ini-ibeheetim@aksu.edu.ng*
[i]*Institute of Corrosion Science and Technology, Guangzhou 510530, China. E-mail: boo@icost.ac.cn*
[j]*Nigerian Alumni Association of the Institute of Metal Research, Chinese Academy of Sciences (NAAIMCAS), Nigeria*
[k]*Africa Center of Excellence in Future Energies and Electrochemical Systems (ACEFUELS), Federal University of Technology, Owerri, Nigeria*
[l]*Department of Industrial Chemistry, Madonna University, Elele, Nigeria*
[m]*Department of Polymer and Textile Engineering, Federal University of Technology, PMB 1526, Owerri, Nigeria*
[n]*Key Laboratory of Advanced Marine Materials, Key Laboratory of Marine Environmental Corrosion and Bio-fouling, Institute of Oceanology, Chinese Academy of Sciences, Qingdao, 266071, PR China*

† Electronic supplementary information (ESI) available. See DOI: https://doi.org/10.1039/d4ra06070a

© 2024 The Author(s). Published by the Royal Society of Chemistry

Open Access Article. Published on 09 October 2024. Downloaded on 7/19/2025 2:17:10 AM. This article is licensed under a Creative Commons Attribution-NonCommercial 3.0 Unported Licence.

different from that of the alloy matrix, resulting in the intermetallic compound being either anodic or cathodic compared to the matrix of the aluminum alloy. This disparity in corrosion potential results in increased susceptibility of the alloy to localized damage by corrosion, hence, micro galvanic corrosion readily occurs by the anodic intermetallic phase dissolution or anodic dissolution of the alloy matrix which is governed by the cathodic function of the intermetallic compound.[8–12]

Micro galvanic corrosion, just like galvanic corrosion kicks in when two different metals come into electrical contact in a conducting medium. The galvanic setup is made up of two different parts which support either anodic or cathodic partial reactions. A convenient way to evaluate the feasibility of galvanic corrosion is to carry out a comparison of the standard corrosion potentials of the intermetallic compound and the matrix in a particular environment. Corrosion is more probable if the difference in corrosion potential between the metals is high. The metal having the lower electrode potential will assume the anode and will dissolve. In contrast, the metal having the greater electrode potential will assume the cathode and support the cathodic processes.

However, the metal corrosion is also affected by some principal factors such as pH, temperature, conductivity, presence or absence of heavy metals, availability of cathodic reactant, and the pitting and corrosion potentials. In the case of Al-alloys, pitting corrosion is always because of chloride ions which occur in operational environments, also the corrosion potential is vital because of the electrochemical nature of most corrosion processes. Furthermore, pH is important in the localized

Alexander I. Ikeuba

Alexander I. Ikeuba is an expert in corrosion science, electrochemistry, and surface science with vast experience in electrochemical methods, spectroscopic methods, material characterization methods and in situ *scanning vibration electrode techniques and computational chemistry. He is a well published researcher with a rapidly growing four-digit citation index and was recently top 2% scientists in the world as published on 16 September, 2024 by Elsevier/Stanford University. He has attended and presented papers in many international conferences. A sought-after conference presenter and reviewer for esteemed publishers (Elsevier, Springer, Emerald, The Electrochemical Society). He is a member of the Royal Society of Chemistry (RSC), American Chemical Society (ACS), and the Chemical Society of Nigeria (CSN).*

Chigoziri N. Njoku

Chigoziri N. Njoku has a PhD in Material Science and Engineering from the University of Chinese Academy of Science, China. He is a faculty member and a senior researcher at the Chemical Engineering Department, and Africa Centre of Excellence in Future Energies and Electrochemical Systems (ACE-FUELS) at the Federal University of Technology, Owerri, Nigeria. His research interests are corrosion protection Technology, optimization, environmental, and chemical engineering.

Okpo O. Ekerenam

Okpo O. Ekerenam is a Lecturer at the Federal University of Technology, Ikot Abasi, Nigeria. He obtained his PhD in Materials Science and Engineering from the University of Chinese Academy of Sciences, China. His research interests include; corrosion protection of materials, nanoscience and technology, and theoretical chemistry.

Demian I. Njoku

Demian I. Njoku earned his PhD in Materials Science and Engineering from the University of Chinese Academy of Sciences in 2018. He holds both an MSc and a BSc in chemistry, specializing in environmental and industrial options, respectively. Currently, he is a research associate at the School of Science and Technology, Hong Kong Metropolitan University. He also held faculty positions at ACEFUELS-FUTO and Madonna University in Nigeria. His research interests include green filters for wastewater purification, microfluidic devices, environmental contaminant assays, computational studies, smart polymeric composites, and corrosion mitigation strategies.

© 2024 The Author(s). Published by the Royal Society of Chemistry

Open Access Article. Published on 09 October 2024. Downloaded on 7/19/2025 2:17:10 AM.
This article is licensed under a Creative Commons Attribution-NonCommercial 3.0 Unported Licence.

corrosion of the aluminum alloys. The pH increases which occurs at cathodic intermetallic compounds increases the corrosion vulnerability of aluminum alloys.[11,12] This indicates that the corrosion potentials may not be reliably used to forecast the intermetallic compounds' electrochemical properties in Al alloys. For example, Mg_2Si possesses a lower corrosion potential than η-phase but unexpectedly displays a much lower corrosive activity than η-phase. Similar inconsistencies have also been noted in the corrosion characteristics of some cathodic phases in Al alloys. For example, Al_3Fe phase possesses higher potential relative to Al_2Cu but shows a lower ability to support cathodic reaction. Hence, the mechanisms of corrosion and the extent localized corrosion damage caused by a particular intermetallic compound cannot be sufficiently described using concepts deduced from the noble or active electrochemical activity of the intermetallic compound.[10–14]

Apart from the electrochemical nature of intermetallic compounds, other variables affect how aluminum alloys corrode locally such as the size of the intermetallic compounds.[3] Pieces of literature on the impact of intermetallic on the localized corrosion of aluminum alloys with different intermetallic phases indicate when the size of the intermetallic compound *e.g.* S-phase is between 2–10 nm, the $Al_{20}Cu_2Mn_3$ assumes the primary function in the localized corrosion propagation, on the other hand, if S-phase has a size bigger than 10 nm, both the S-phase and $Al_{20}Cu_2Mn_3$ actively contribute to the localized corrosion features of the alloy matrix.[5,12]

Many corrosion mitigation strategies have been developed to control the corrosion of alloys,[15–29] however, to gain more understanding of the corrosion of aluminum alloys, an understanding of the role of intermetallic compounds in the localized corrosion of the alloy is needed.[1–5]

2 Intermetallic particles (second phases) in aluminum alloys

A variety of intermetallic compounds are produced by different alloying components and impurities in aluminum alloys. They are

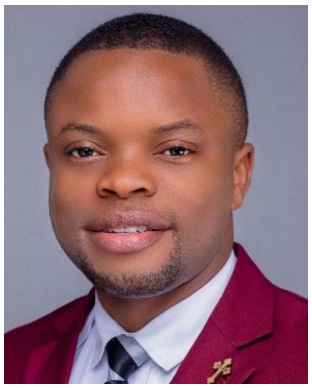

Inime I. Udoh

Inime Udoh has a PhD in Materials Science and Engineering from the University of Chinese Academy of Sciences. He is currently a postdoctoral fellow at The Hempel Foundation Coatings Science and Technology Center (CoaST), Department of Chemical and Biochemical Engineering, Technical University of Denmark. His research focuses on corrosion science and protection, with emphasis on the application of smart nano/microcontainers for the fabrication of functional organic coatings.

Enobong F. Daniel

Enobong Daniel holds a PhD in Material Science and Engineering from the University of Science and Technology of China, China. She is currently a postdoctoral researcher at the Institute of Metal Research, Chinese Academy of Sciences, China. Her research focuses on corrosion monitoring and protection of materials.

Paul C. Uzoma

Paul Chinonso Uzoma is a postdoctoral researcher at Zhejiang University – University of Illinois Urbana Champaign, Haining, China. He holds a PhD in Material Science and Engineering from the University of Science and Technology of China (USTC). He has been actively engaged in research for more than a decade. His research focus is on nanomaterials and surface coatings for corrosion protection, anti-ice, self-cleaning, self-healing and nanotribology.

Ini-Ibehe N. Etim

Dr Ini-Ibehe Nabuk Etim is a Visiting Ass. Professor at Institute of Oceanology, CAS. He was the former Ag. Head, Department of Marine Science, Akwa Ibom State University, Nigeria (2021–2024). He is also a facilitator at the Africa Centre of Excellence for Future Energies and Electrochemical Systems (ACE-FUELS), FUTO, Nigeria. He recently won a grant from the prestigious CAS President's International Fellowship Initiative (PIFI) as a High Talent Visiting Scientist in 2023. He's an awardee of the Chinese Government Scholarship, CSC (2015). He is an ARIFA postdoctoral fellow at the Federal University of Santa Catarina (UFSC), Florianopolis, Brazil.

Open Access Article. Published on 09 October 2024. Downloaded on 7/19/2025 2:17:10 AM.
This article is licensed under a Creative Commons Attribution-NonCommercial 3.0 Unported Licence.

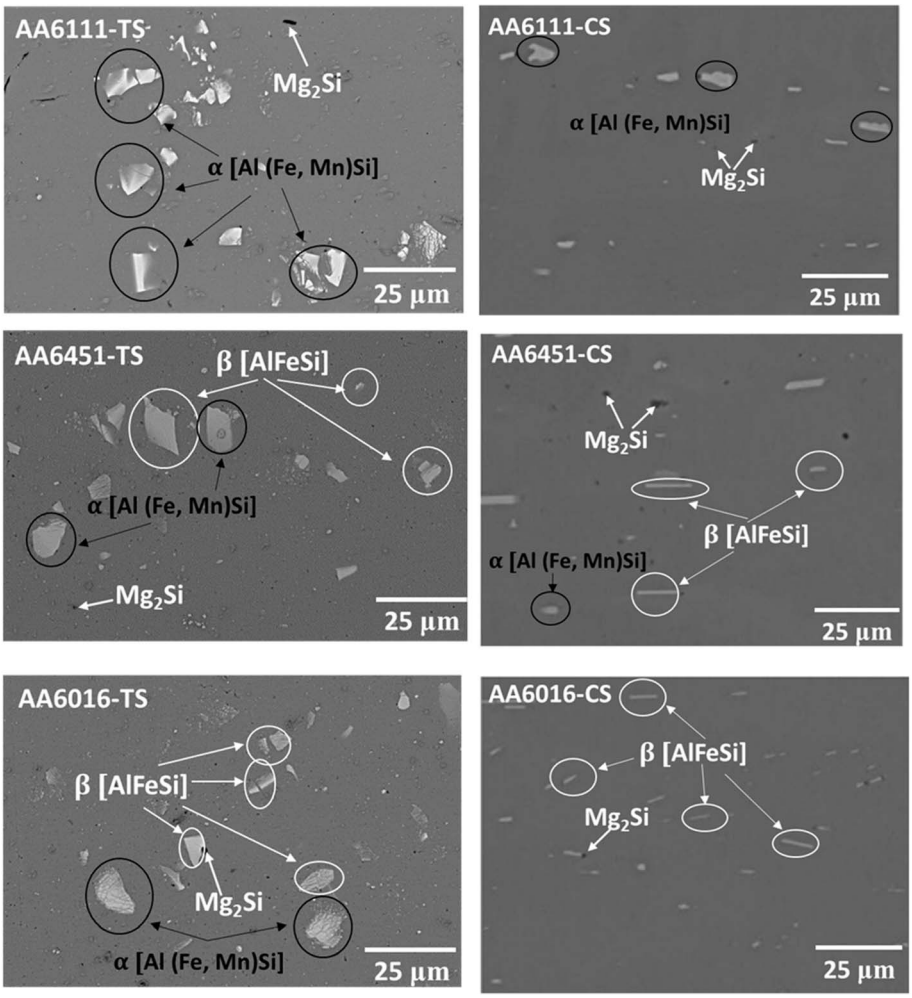

Fig. 1 SEM images of the polished top surfaces and cross-sections of the AA6*xxx*. The Al-matrix is dark and dispersed with bright IMPs. EDS analysis of AA6*xxx* reveals Mg_2Si and α IMPs in AA6111, while α, β and Mg_2Si were identified in AA6451 and AA6016. The α IMPs are blocky, the Mg_2Si particles are dark and β IMPs are two-dimensional plate/needle-like structures. This figure has been adapted/reproduced from (ref. 29) with permission from Sringer Nature, copyright 2024.

classified into four groups namely, precipitates, constituents, dispersoids, and primary particles.[5,7] Precipitates are defined as second phases formed during the process of heat treatment below the solidus line, they improve the strength of alloys. Coarse precipitates are mostly found at the sub-grain or grain boundaries. Al-alloys with high mechanical properties often contain precipitates like (Al_2CuLi), δ (Al_3Li), η-phase, Q ($Al_4Cu_2Mg_7Si_8$), β-phase, θ (Al_2Cu), and Mg (Zn, Cu, Al)$_2$. Dispersoids are defined as microscopic second phases that are almost insoluble in Al. These intermetallic compounds are often formed from Al and transition metals like Cr, Mn, and Zr. Dispersoids improve the toughness of the alloy matrix by suppressing recrystallization or limiting the movements of grains. Examples of dispersoids include $Al_{20}Cu_2Mn_3$, $Al_{12}Mn_3Si$, $Al_{12}Mg_2Cr$, Al_3Zr, and Al_6(Fe, Mn). Constituents are defined as intermetallic compounds that are generated by eutectic processes during solidification. These particles are mostly Fe, Si, and other low solubility alloying elements for example, Al_3Fe, Al_6Fe, Al_6Mn, Mg_2Si, $Al_{12}(FeMn)_3Si$, Al_6(Fe, Cu), and Al_7Cu_2Fe.[8] The size of the constituents usually mostly varies between 1–30 μm. Primary particles are defined as intermetallic compounds with a different phase formed in addition to the solid aluminum solution. Si- and Fe primary particles are commonly formed by 4*xxx* and 8*xxx* alloys, respectively.[5–12]

3 Factors that affect the impact of intermetallic particles on the localized corrosion of aluminum alloys

In aluminum alloys, the presence of intermetallic particles can significantly alter how well they resist corrosion. Composition, distribution, and electrochemical behavior are the three key elements that can be used to classify the parameters influencing how these particles impact corrosion.

3.1 Composition

The chemical composition influences intermetallic particle corrosion behavior. When compared to the surrounding aluminum matrix, these particles frequently have a different composition, which causes galvanic coupling and localized corrosion.

© 2024 The Author(s). Published by the Royal Society of Chemistry

Open Access Article. Published on 09 October 2024. Downloaded on 7/19/2025 2:17:10 AM.
This article is licensed under a Creative Commons Attribution-NonCommercial 3.0 Unported Licence.

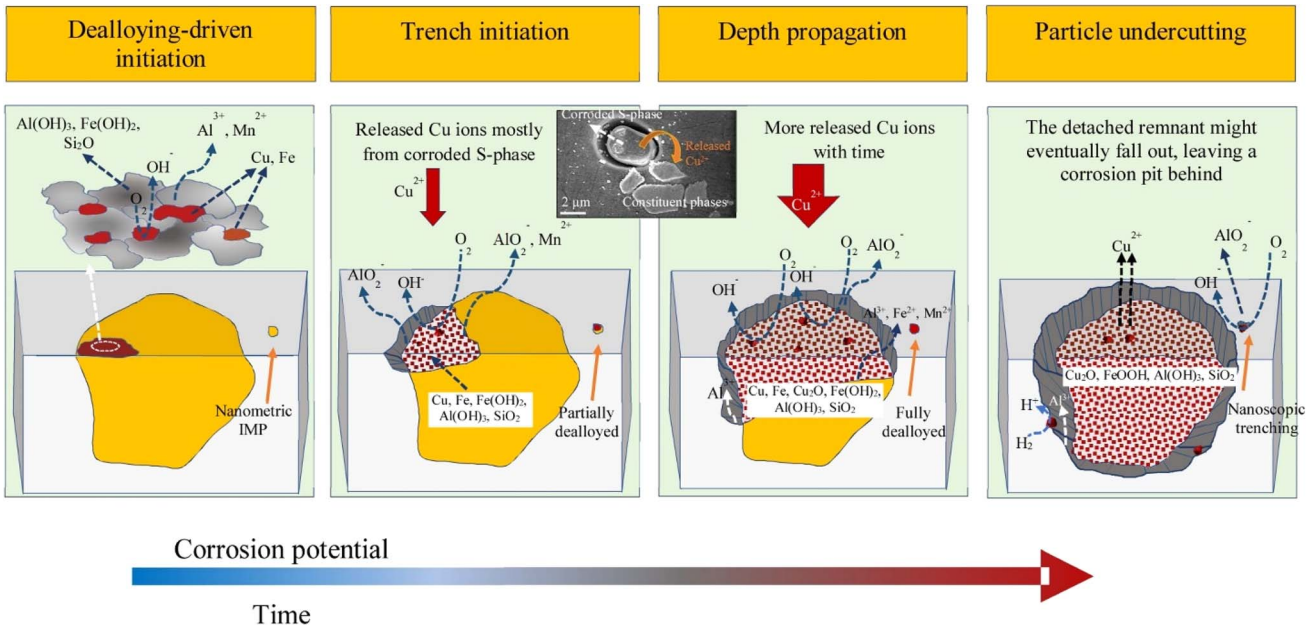

Fig. 2 Schematic presentation of localized corrosion initiation induced by cathodic dispersoids and constituent phases. The envisaged reactions are shown, the initiation sites are the IMPs thereafter propagation, trenching and depth propagation sets in the vicinity of the matrix through galvanic interactions. The post corroded sample is indicated in the inset above the scheme revealing Cu released from a dealloyed Al_2CuMg and redeposited on other IMPs and the surrounding alloy matrix. This figure has been adapted/reproduced from (ref. 31) with permission from Elsevier, copyright 2024.

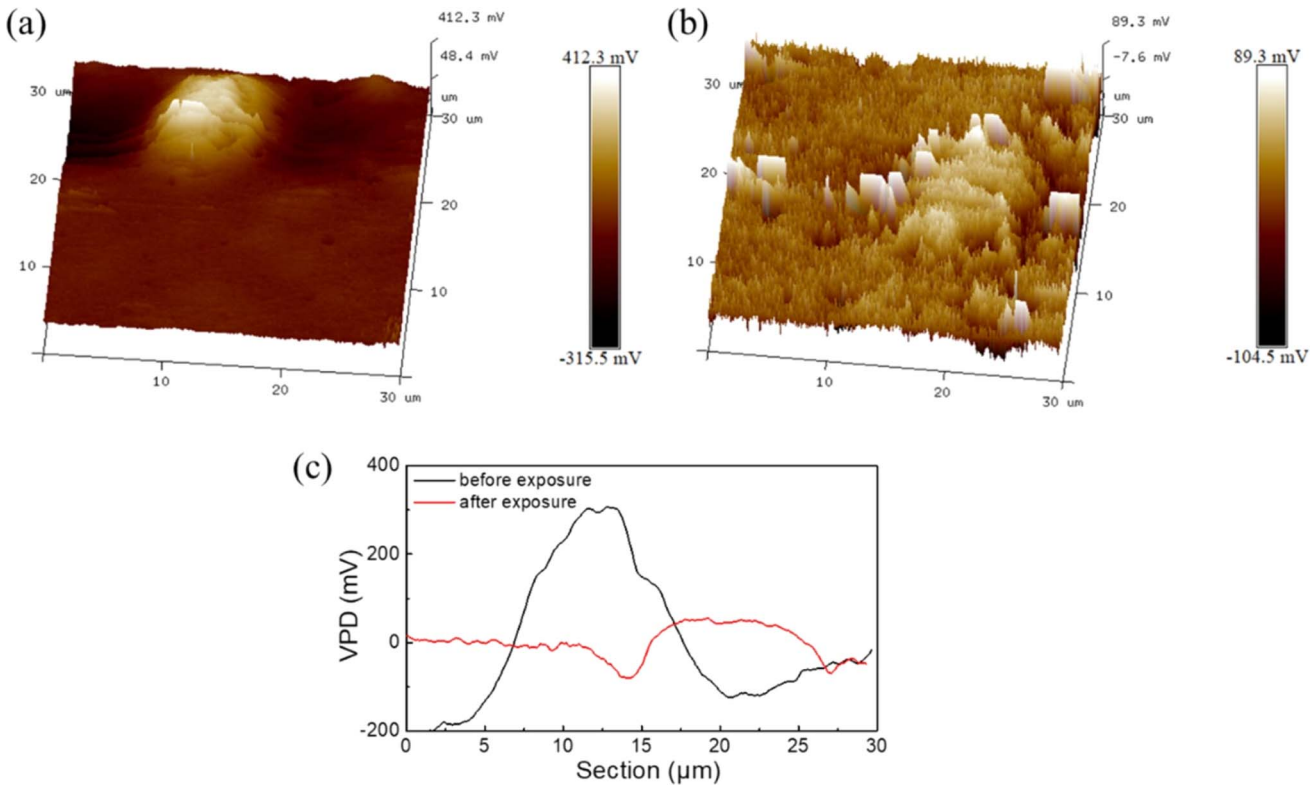

Fig. 3 The VPD of Al–Mn and α-Mg in AM50 (a) before corrosion, (b) after corrosion and (c) corresponding line-profile analysis of relative potential through the secondary phases. This figure has been adapted/reproduced from (ref. 32) with permission from Elsevier, copyright 2024.

Open Access Article. Published on 09 October 2024. Downloaded on 7/19/2025 2:17:10 AM.
This article is licensed under a Creative Commons Attribution-NonCommercial 3.0 Unported Licence.

Intermetallic particles, which can have a variety of chemical compositions, such as Al–Mg, Al–Si, Al–Cu, or Al–Fe, among others, are frequently found as second phases in aluminum alloys. Mg_2Si, AlFeSi and Al(FeMn)Si are examples of intermetallic phases (IMPs) with different compositions that promote localized corrosion (Fig. 1). The IMPs are seen to occur in varied sizes and distribution and affect the alloy corrosion in numerous ways.

3.2 Galvanic effects

Galvanic couplings can form inside the aluminum matrix due to the presence of dissimilar metals or alloys in the intermetallic particles. The galvanic interaction of intermetallic particles with aluminum can either raise or decrease how quickly the alloy corrodes, based on the makeup of each. Localized corrosion is promoted around the IMPs when parts of more noble IMPs in the Al alloy give it a higher cathodic potential than the Al matrix and are subjected to corrosive conditions.[30] Kosari *et al.*[31] investigated local corrosion in aluminum alloys by TEM using combined quasi-*in situ* and *ex situ* analysis and found that dealloying of dispersoids and component phases catalyzes corrosion. Dealloyed components of IMPs cause the nearby alloy matrix to dissolve locally (Fig. 2). In addition, the inherent electrochemical instability of intermetallic compounds plays a significant role in local deterioration, which results from galvanic contacts between the adjacent alloy matrix and the dealloyed sections of the IMPs.

3.3 Micro galvanic effects

The composition of intermetallic particles might vary even within a single particle. Localized corrosion can result from these compositional changes because they can produce micro galvanic cells within the particle itself. What makes up the intermetallic particles determines the degree and severity of micro galvanic corrosion.[32] For example, the volta potential plots across Al–Mn

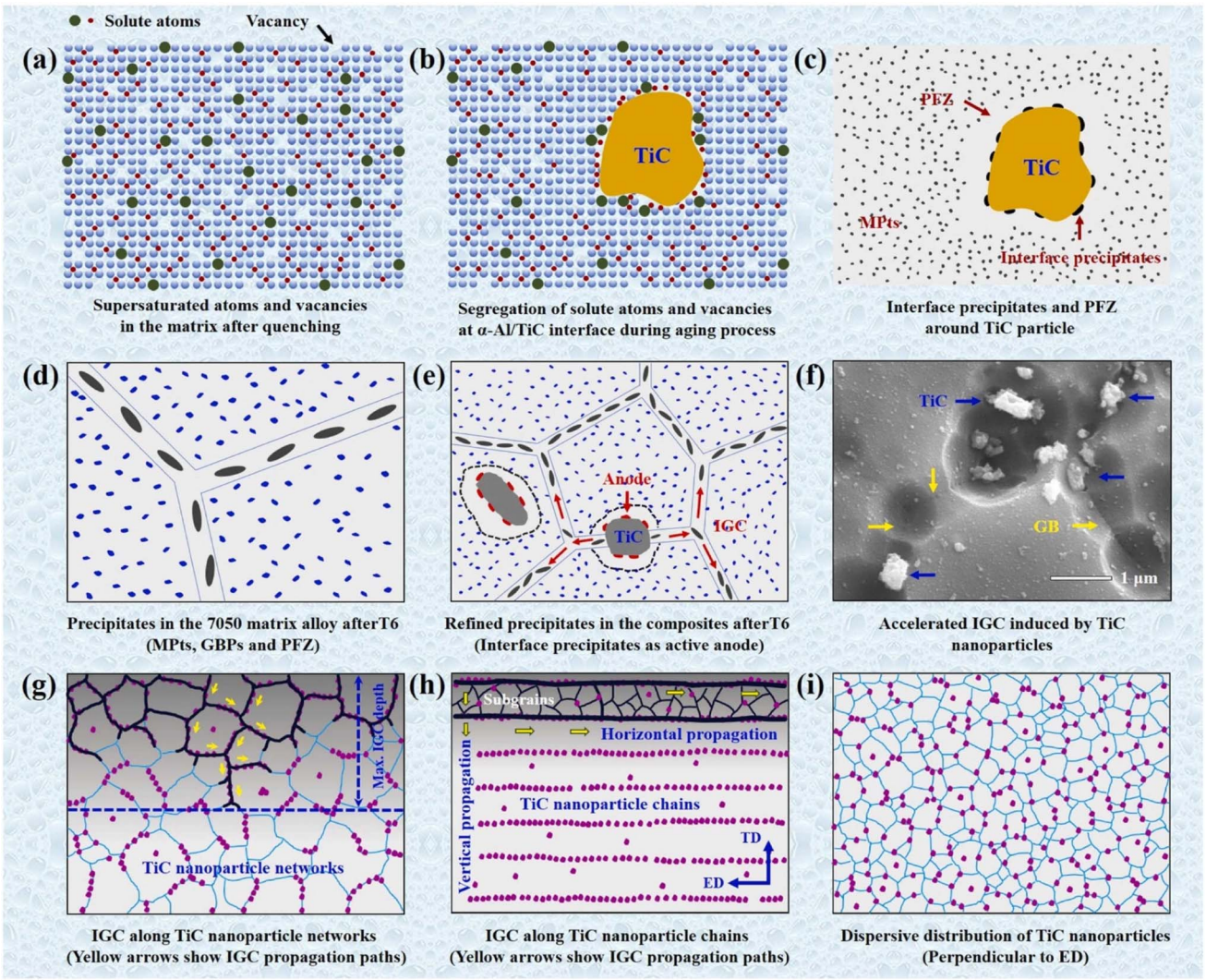

Fig. 4 Schematic of interface precipitation and corrosion mechanisms in Al–Zn–Mg–Cu aluminum alloy composite: (a–c) preferential segregation of precipitates at the α-Al/TiC interface; (d and e) difference in aging kinetics between alloy and composites; (f) initiation and propagation of IGC in composites (g–i) IGC susceptibility to TiC particles distribution configurations. This figure has been adapted/reproduced from (ref. 34) with permission from Elsevier, copyright 2024.

© 2024 The Author(s). Published by the Royal Society of Chemistry

Open Access Article. Published on 09 October 2024. Downloaded on 7/19/2025 2:17:10 AM. This article is licensed under a Creative Commons Attribution-NonCommercial 3.0 Unported Licence.

and α-Mg in AM50 shows a wide variation in potentials indicating different tendencies toward anodic and cathodic behavior (Fig. 3). Additionally, the potential difference in the local environment and the necessity for a galvanic driving force to initiate the anodic dissolution. Therefore, local corrosion mostly spreads *via* the micro-galvanic impact of the nanoscale, which is brought on by the dealloying process. By affecting the localized electrochemical response, the IMP microstructure influences the beginning of corrosion in aluminum alloys, which highlights the importance of managing IMPs.[32]

3.4 Precipitation reactions

Some intermetallic particles may serve as sites where corrosion-related phases precipitate. For instance, when exposed to aqueous environments, the intermetallic phase Mg_2Al_3 in Al–Mg alloys can function as a nucleation site for the precipitation of the corrosion product $Mg(OH)_2$. These precipitates may modify the ionic and pH concentrations in the area, which may change how corrosion behaves nearby. Precipitate aggregation events in an AA6061 microstructure that has partially recrystallized were better-understood thanks to Ly and coworkers.[33] According to their findings, particle segregation causes shear bands in aluminum alloys with ultra-fine grains to be favored locations for pitting and intergranular corrosion. However, TiC particles strengthened Al–Zn–Mg–Cu aluminum alloy model was investigated with respect to interface precipitation and corrosion mechanisms.[34] The initiation and propagation of intergranular corrosion were observed to emerge from selective dissolution of interface precipitates on the alloy matrix which serve as probable sites for corrosion product deposition (Fig. 4).

3.5 Particle size

The size and distribution of IMPs in the alloy matrix influence corrosion behavior as well. Fine and uniformly scattered particles can provide more effective corrosion resistance by blocking the movement of corrosive species and serving as physical barriers. Larger or grouped particles, however, could create localized corrosion cells and facilitate the propagation of corrosion.[35] Kayani *et al.* (2024) carried out an investigation on the impact of intermetallic phases on the localized pitting corrosion and high-temperature tensile strength of Al–SiMg-CuNi alloys.[36] It was discovered that the degree and spread of volta potential depended on the size of the IMP which contained phases such as γ-Al_7Cu_4Ni, δ-Al_3NiCu, and Q-$Al_5Cu_2Mg_8Si_6$ (Fig. 5).

3.6 Alloy microstructure

The microstructure of the aluminum alloy, including grain size, phase distribution, and segregation affect the dissolution behavior of IMPs. These microstructural features have the power to modify the accessibility of corrosive species to the alloy surface as well as the availability of corrosion pathways, which can affect how susceptible the alloy is to corrosion. Xiao *et al.* examined the microstructure and intergranular corrosion behavior of 2024 alloy with varying Cu and Mg content using a three-dimensional atom probe and scanning and transmission electron microscopy (SEM and TEM).[37] The findings demonstrate that following quenching, nanoscale θ (Al_2Cu) and S (Al_2CuMg) particles precipitate at grain boundaries. It was found that the presence of θ (Al_2Cu) and S (Al_2CuMg) phases in the region of grain boundaries has a significant impact on how susceptible it is to intergranular corrosion. As local cathodes,

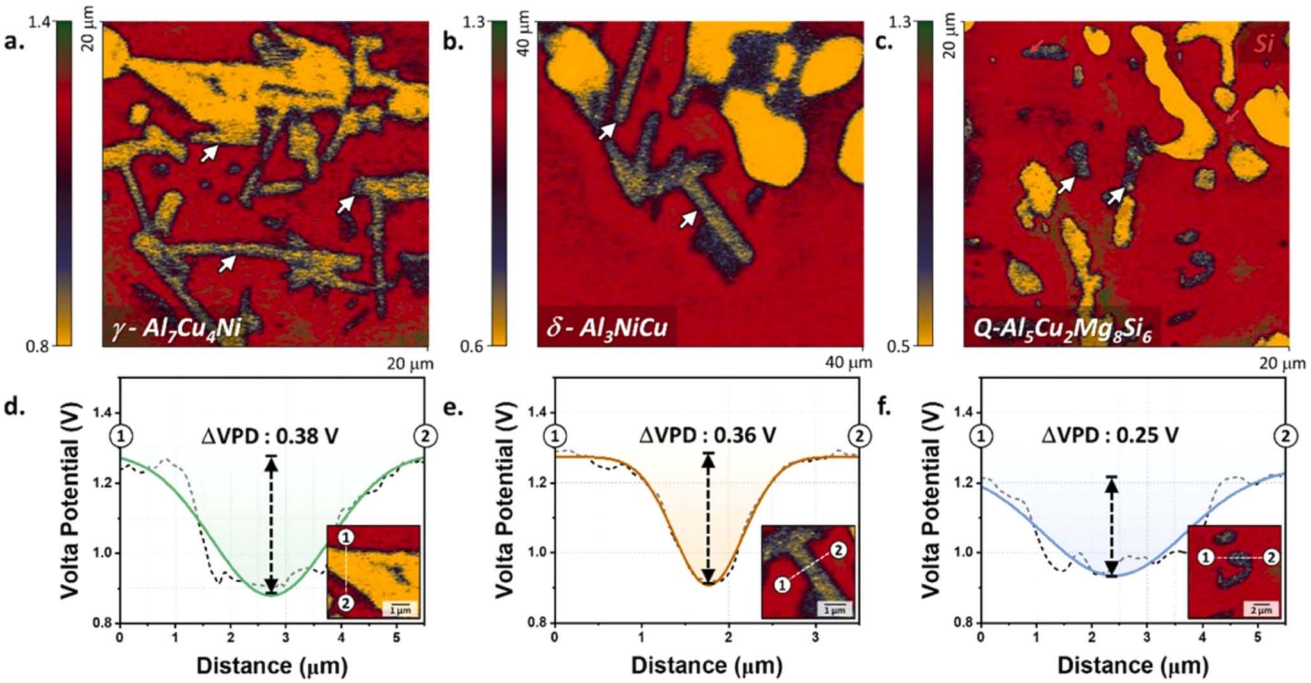

Fig. 5 Volta potential maps (insets) and line profiles of (a, d) γ-Al_7Cu_4Ni, (b, e) δ-Al_3NiCu, and (c, f) Q-$Al_5Cu_2Mg_8Si_6$ phases in T6-treated aluminum alloy. This figure has been adapted/reproduced from (ref. 36) with permission from Elsevier, copyright 2024.

Open Access Article. Published on 09 October 2024. Downloaded on 7/19/2025 2:17:10 AM. This article is licensed under a Creative Commons Attribution-NonCommercial 3.0 Unported Licence.

intermetallics and Cu-rich precipitates promote oxygen reduction and, in turn, anodic dissolution of the matrix material in their surroundings. In another report,[36] the microstructural evolution of a T6 treated Al-alloy was provided (Fig. 6). Distinct phases were identified from the backscattered images such as Mg_2Si, Q-phase, Ni-rich IMPs among others. The variation in microstructural features was noted to impact the corrosion behavior of the alloy.

3.7 Distribution

The impact of intermetallic particles on corrosion depends on how they are distributed inside the aluminum alloy. A corrosion attack may be more homogeneous if particles are equally dispersed throughout the matrix. Localized corrosion, as that found in crevice or pitting, can happen if the particles group together or create galvanic couples with the nearby aluminum matrix. For example, factors considered in a work on Al–Mg–Si alloy include the nature and distribution of intermetallics linked to corrosion potential, pitting potential, current density, ultimate tensile strength, and elongation.[38] Primary dendritic and cellular spacings were also elucidated. A dendritic zone that appeared for cooling rates with values less than 0.8 K s^{-1} was found after the high cooling rate cellular region. The major dendritic arm spacing ranged from 120 m to 270 m, but the cellular spacing ranged from around 16 m to 38 m. It was demonstrated that the Mg_2Si and Fe-containing particles in the Al cellular zone are finely dispersed, which improved the mechanical characteristics (strength and elongation) and affected corrosion resistance. For 0.15 M and 0.5 M NaCl electrolytes, it is shown that the scale of $\lambda = 1$ within the dendritic zone has no impact on mechanical strength or corrosion resistance. An illustration of an IMPs size analysis is shown in Fig. 7. It seen that the size and area of the intermetallic particles differ greatly.

3.8 Electrochemical behavior

The corrosion impact of IMPs is also influenced by their electrochemical characteristics, such as their nobility or activity in the presence of corrosive conditions. Noble intermetallic phases have the potential to function as cathodic sites and hasten

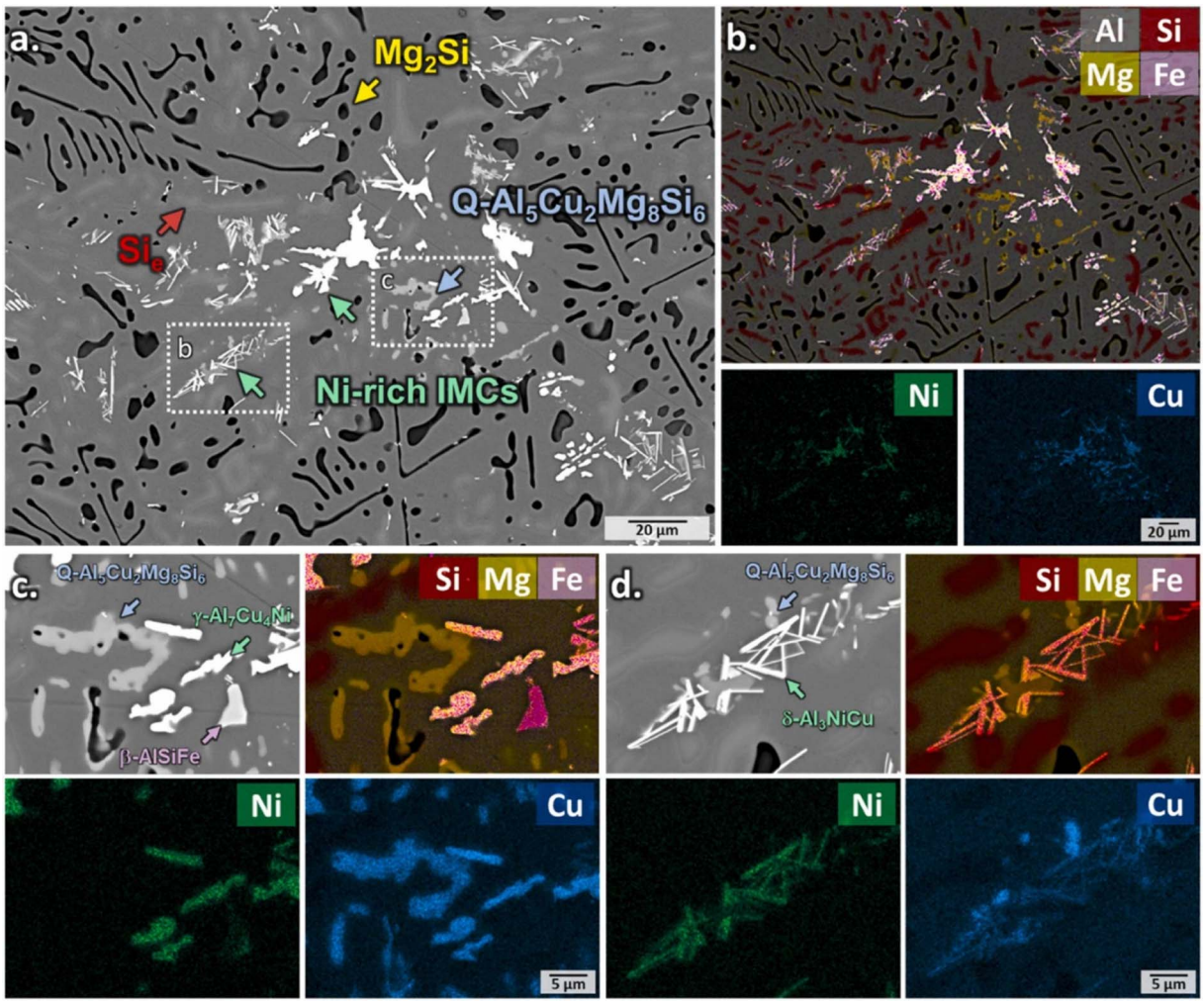

Fig. 6 (a) BSE images and (b) EDS elemental maps of Al single bond Si single bond Mg single bond Cu single bond Ni alloys after T6 treatment. High-magnification BSE images and corresponding EDS elemental maps of (c) γ-Al_7Cu_4Ni and (d) δ-Al_3NiCu phases.[36] This figure has been adapted/reproduced from (ref. 36) with permission from Elsevier, copyright 2024.

© 2024 The Author(s). Published by the Royal Society of Chemistry

Open Access Article. Published on 09 October 2024. Downloaded on 7/19/2025 2:17:10 AM.
This article is licensed under a Creative Commons Attribution-NonCommercial 3.0 Unported Licence.

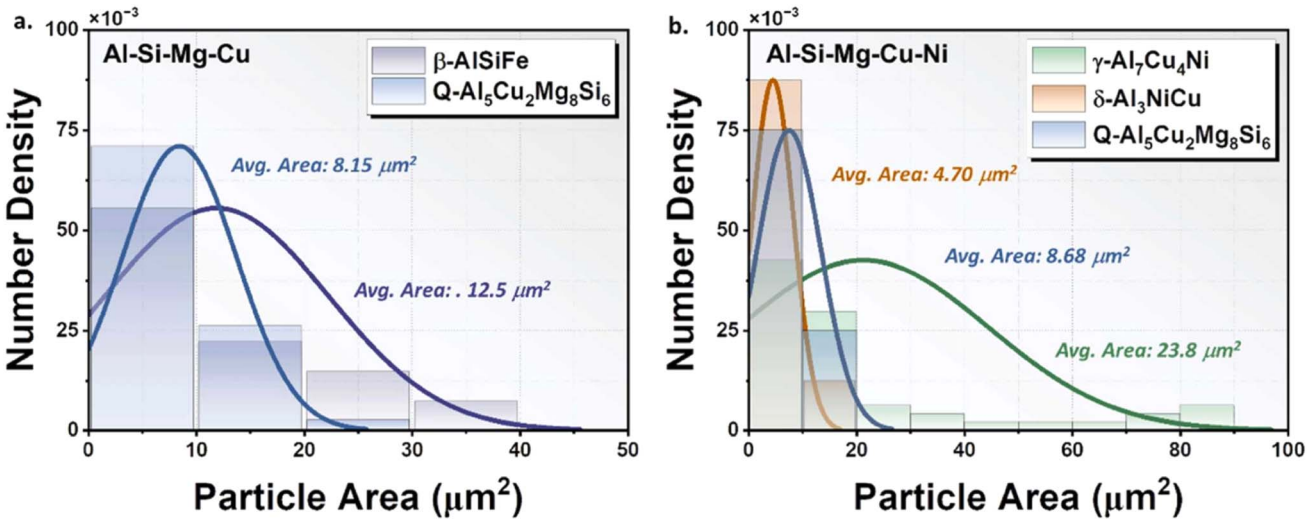

Fig. 7 IMP size/area analysis in (a) Al single bond Si single bond Mg single bond Cu and (b). Al single bond Si single bond Mg single bond Cu single bond Ni alloys under T6 conditions. The phases present are the β-AlSiFe and Q-$Al_5Cu_2Mg_8Si_6$, and γ-Al_7Cu_4Ni, δ-Al_3NiCu, and Q-$Al_5Cu_2Mg_8Si_6$. This figure has been adapted/reproduced from (ref. 36) with permission from Elsevier, copyright 2024.

aluminum matrix degradation. On the other hand, more active particles can experience preferential corrosion, sacrificially defending the aluminum matrix. Fig. 8 portrays a range of corrosion potentials for some IMPs, the higher the corrosion potential, the greater the tendency towards cathodic reactions. Li *et al.*[39] used a microelectrochemical cell technique, fast Fourier transform to measure the impedance of intermetallic particles in the matrix of AA2024-T3. The *in situ* measurement of capacitance evolution was used to track the dealloying of the S-phase. An uncomplicated Randles circuit was used to explain how intermetallic particles interacted with NaCl and chromate solutions. Al_2CuMg (S-phase) had the highest dissolving propensity, according to impedance analysis and anodic polarization, as opposed to net cathodes in the other phases. Moreover, according to a work by Wang *et al.*,[40] transmission electron microscopy has shed light on the size-dependent electrochemical implication of the activity of the S phase during the early stages of corrosion in the 2024 Al alloy. Upon

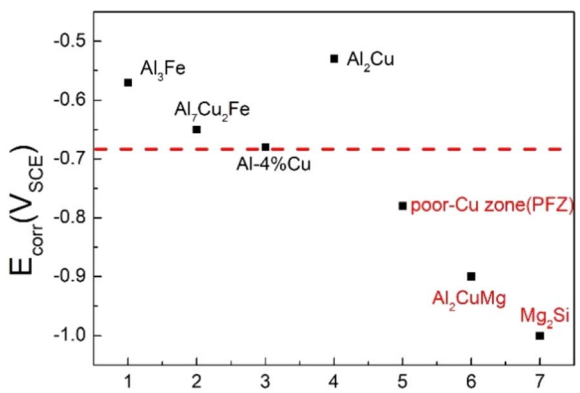

Fig. 8 The electrode potential IMPs in of 2024-T3 aluminum alloy. This figure has been adapted/reproduced from (ref. 37) with permission from MDPI, copyright 2024.

onset of corrosion, when $Al_{20}Cu_2Mn_3$ dispersoids are vital, a critical size of roughly 10 nm is found below which S phases are incapable of performing electrochemical functions. The local deterioration of the Al matrix is initiated by the electrochemical implications of S phases, which become more prominent as the size gets bigger.

In addition to these factors, it is worthy of note that smaller particles with a larger surface area relative to their volume can promote more localized corrosion due to enhanced electrochemical activity. Moreover, contact potential difference is another critical factor that affects the effect of IMPs on the deterioration of Al alloys. In a work by Liew and co-workers,[41] scanning Kelvin probe force microscopy (SKPFM) was adopted to monitor the local contact potential difference (VCPD) in real-time while conducting an *in situ* assessment on the micro-galvanic interactions that occur during chloride-induced corrosion between aluminum alloy AA2099's alloy matrix and aluminides that comprise Cu, Fe, Mn, and Li. When the matrix was surrounded by an aluminide cluster, the aluminides displayed noble potential and could ennoble the surrounding matrix sites. As a result, the matrix changed to a more favorable VCPD toward the aluminides. Throughout the corrosion exposure, the anode-to-cathode ratio was altered and was observed to have a dynamic nature. When the surface of Al–Li AA2099 initially interacted with high humidities, far higher local VCPD activities were noticed than in later RH cycles; this behavior was not observed in other aluminum alloys. It is crucial to remember that a variety of variables, including alloy composition, production conditions, exposure environment, and surface treatments, interact in a complex way to determine how aluminum alloys will behave regarding corrosion. To anticipate and manage the corrosion performance of Al alloys, it is crucial to comprehend the unique properties of intermetallic particles and how they interact with the aluminum matrix.

Open Access Article. Published on 09 October 2024. Downloaded on 7/19/2025 2:17:10 AM.
This article is licensed under a Creative Commons Attribution-NonCommercial 3.0 Unported Licence.

Table 1 Collection of techniques for characterizing the electrochemical behavior of intermetallic particles of Al-alloys

S/N	Al alloy	Method	Description	Results	References
Electrochemical techniques					
1	Al–Zn–Mg alloy	Polarization method	The precipitation hardening treatment influences the corrosion of the material and the efficacy of the sacrificial anode		71
2	$MgZn_2$ intermetallic compound	Electrochemical impedance spectroscopy (EIS) and polarization method	Polarization data showed the nature of film formed upon exposure of the matrix in different pH conditions	This part formed a different mechanism for the dissolution of the $MgZn_2$ material	72
3	The characterized $MgZn_2$ particle coupled with Al	The scanning vibrating electrode technique (SVET), and the scanning ion-selective electrode technique (SIET)	Local alkalization within $MgZn_2$ was revealed by SIET utilizing the H^+ and Cl^- ion distribution maps	Findings show that the dissolution of $MgZn_2$ leads to Mg saturation in the outer film and Zn addition on the material surface	73
4	The galvanic corrosion between the Q-phase/Al couple	SIET and SVET methods	SVET data reveal that the anodic oxidation process of Al was initiated to understand the corrosion process in alkaline pH (pH 13) but proceeded *via* a localized manner in low pH media (pH 2 and 6)	The Al anodic dissolution in the Q-phase/Al couple is pH dependent while the galvanic polarity is independent of pH	74
5	$Al_4Cu_2Mg_8Si_7$	The influence of pH on the corrosion of material	EIS method	The extent of the EIS components (R_{ct} and R_f) regarding the Q-phase varied with pH. The magnitude at intermediate acidic pH was higher compared to very low acidic and very high pH alkaline indicating better protection at neutral pH conditions	75
Microscopic techniques					
6	$Al_{2.23}Cu_xLi$	TEM and SEM methods	Microstructure analysis	The imaging techniques revealed the entire corrosion process along the {111} Al planes	76
7	Al–Cu alloy with different crystal orientations	SEM and TEM	Investigating the corrosion behaviors of alloys with different crystal orientations *i.e.* (111), (001), and (101)	The imaging data complemented by the EIS technique show that corrosion rates differ with orientation and in alloy without precipitates, the corrosion resistance was known by the atomic density of the crystal structure	77
8	$AlSi_1Mg$ alloy	SEM, TEM, and EDX	The study of composition and morphology properties of the intermetallic phases in $AlSi_1Mg$ alloy	The elemental and microscopic techniques reveal the intermetallic features of the aluminum series which depends on composition and cooling rate	78

© 2024 The Author(s). Published by the Royal Society of Chemistry

Open Access Article. Published on 09 October 2024. Downloaded on 7/19/2025 2:17:10 AM.
This article is licensed under a Creative Commons Attribution-NonCommercial 3.0 Unported Licence.

Table 1 (*Contd.*)

S/N	Al alloy	Method	Description	Results	References
9	Cast $AlSi_5Cu_1Mg$ and $AlCu_4Ni_2Mg_2$ aluminum alloys	Optical light microscopy (OLM), SEM with EDS and XRD to identify intermetallic in the alloys	Characterize surface morphologies and extent of the microstructure intermetallic phases in cast aluminum	While the microscopic methods reveal the distribution of the intermetallic particles, EDS reveals the elemental composition and XRD reveals the phases of the intermetallic particles	79
10	$AlSi_5CuMg$ alloy	DSC	The investigation led to the understanding of the intermetallic components in Al	DSC curves probe the reaction process of as-cast alloy	80
11	$AlSi_5Cu_2Mg$ cast alloy	OM, SEM, and TEM	Microstructural examination	These techniques reveal the three intermetallic α-AlFeMnSi phase precipitates which varied morphologically and in chemical compositions. The shapes were related to the conditions of the crystallization process	81
Thermal and spectroscopic techniques					
12	Mg_2Si intermetallic	DSC	DSC provides the liquid fraction of the alloy and the increasing density with holding time	DSC reveals the uniform spheroidization of the semi-solid processed aluminum matrix	82
13	$Al_{84}Ni_7Co_3Dy_6$ bulk specimen	DSC and XRD	The role of precipitation within intermetallic phases through crystallization	DSC curve of the Al–Co–Ni–Dy particle revealed the endothermic peak and other processes as depicted in the various characterization methods	83
14	$AlCu_2$ at alloy sample	XPS characterization	The XPS was adopted to analyze the thickness and structure within the interfacial oxides of an $AlCu_2$ alloy sample	XPS reveals the extent of covering of the intermetallic particles by the oxides of Al and Cu and Al matrix by aluminum oxide	84

© 2024 The Author(s). Published by the Royal Society of Chemistry

Open Access Article. Published on 09 October 2024. Downloaded on 7/19/2025 2:17:10 AM. This article is licensed under a Creative Commons Attribution-NonCommercial 3.0 Unported Licence.

4 Methods used in the identification and evaluation of the electrochemical behavior of intermetallic particles in the context of Al alloys

4.1 Methods used in characterizing the behavior of intermetallic particles of Al-alloys

Aluminum alloys are achieved by combination of different elements such as iron, copper, and silicon to achieve desired or certain properties required in special applications like in aviation. However, it is also pertinent to understand how the precipitated intermetallic components because of the different elements in the structure affect the electrochemical behavior of the material based on microstructural and electrochemical analysis. The identification and imaging of the intermetallic phases are integral parts of complex investigation of any alloy of interest.[42,43] Combined, calorimetric, microscopic, spectroscopic, and electrochemical methods have been mostly employed in this regard which have assisted in divulging the corrosion potentials and the location of the structure dissolution within the precipitate of the matrix. The microscopic methods include atomic force microscopy (AFM), scanning electron microscopy (SEM), transmission electron microscopy (TEM), optical microscopy (OM), and their derivative. Typical images of results from some notorious microscopic methods are collated in Fig. 1. Spectroscopy methods include X-ray photoelectron spectroscopy (XPS), X-ray analysis (EDS), and X-ray diffraction spectroscopy (XRD).[42–46] Thermal techniques like the DSC (differential thermal calorimetry) were adopted to characterize intermetallic compounds in Al material. The corrosion of alloys depends on the nature of the intermetallic compounds and is usually seen as cathodic within the aluminum structure. These methods have also been employed in other areas of corrosion research.[47–59] Furthermore, severally electrochemical characterizations were adopted to correlate with intermetallic microstructures and the corrosion breakdown of Al materials.[60–65] Electrochemical methods elucidate the effect of intermetallic compounds and their corrosion features.[66–70] Table 1 collated the various methods used in analyzing the intermetallic corrosion properties of aluminum alloys including notorious electrochemical methods, microscopic methods, spectroscopic techniques, and thermal characterizations.

5 Electrochemical characteristic of intermetallic particles in aluminum alloys

The electrochemical behavior of intermetallic particles in aluminum alloys is a complex phenomenon that can have significant effects on the material's properties. Understanding this electrochemical characteristic of intermetallic particles is necessary for developing aluminum alloys that have enhanced corrosion resistance and other desirable properties. For intermetallic particles in aluminum alloys, electrochemical behavior could influence the corrosion process and other characteristics of the material. When an aluminum alloy containing intermetallic particles is exposed to an electrolyte (a solution containing ions), an electrochemical reaction can occur between the alloy and the electrolyte. During the electrochemical reaction, some areas of the alloy can become cathodic (negatively charged) while others can become anodic (positively charged). The intermetallic particles within the alloy can also act as cathodic or anodic sites, depending on their composition and morphology. If an intermetallic particle is cathodic, it can attract the positively charged ions in the electrolyte and reduce the local corrosion rate around the particle. This can protect the adjacent alloy matrix from corrosion. On the other hand, if an intermetallic particle is anodic, it can attract the negatively charged ions in the electrolyte and initiate localized corrosion around the particle. The electrochemical characteristics of intermetallic components could also be influenced by the surrounding environment, such as the pH of the electrolyte, the temperature, and the presence of other ions.[85–88] For example, in a saline environment, chloride ions can increase the anodic behavior of intermetallic particles, leading to pitting corrosion.[89]

There are numerous and diverse intermetallic particles that can develop in aluminum alloys. Some of the common IMPs within the structure of the 7*xxx* series are S phase, Mg_2Si, (Al_2CuMg), θ phase (Al_2Cu), Al_3Fe, (Al, Cu)$_6$(Fe, Cu) and Al_7Cu_2Fe. Particularly, Al_7Cu_2Fe and (Al, Cu)$_6$(Fe, Cu) are prevalent and of great interest within the galvanic interface in the alloy structure.[90,91] Others include, $MgZn_2$, $Al_{20}Cu_2Mn_3$, $Al_{12}Mn_3Si$, $Al_{12}Mg_2Cr$, Al_6Mn, Al_3Ti, Mg(AlCu), Al_6Zr, $Al_{32}Zn_{49}$, and Mg_2Al_3.[88,92] In terms of electrochemical activity, studies have shown that IMPs having Ti, Fe, and Cu, are nobler compared to matrix or pure Al. Examples of such are Al_3Ti, Al_3Fe, Al_2Cu, and Al_7Cu_2Fe. These compounds have a distinctive breakdown potential, demonstrating their ability to support a passive film. The IMPs do not exhibit any breakdown potential and are highly susceptible to corrosion at potentials above their E_{corr}.[92] It is noted that the presence of some of these elements could predict a galvanic cell, especially between matrix and particles, but not an adoptable technique for understanding the characteristics of the elemental particle[91] this is due to the possibility of polarity reversal in certain cases. For example, it was seen that the Mg-rich components, like Mg_2Si, could alter the electrochemical characteristics in the cathodic and anodic parts because of the heat treatment.[85]

Specific work has been conducted to reveal the electrochemical behavior of some of the IMPs present in aluminum alloys. Birbilis *et al.*[90] studied the electrochemical characteristic and corrosion linked with Al_7Cu_2Fe alloys in aluminum material and reported that Al_7Cu_2Fe was cathodic to the structure of other alloys. They further revealed that this IMP could sustain oxygen reduction responses within a range of potentials in NaCl medium within different pH and concentrations. They observed a pitting behavior which was attributed to the presence of Al_7Cu_2Fe. Mallinson *et al.*[91] also identified Al_7Fe_2Cu alongside (Al, Cu)$_6$(Fe, Cu) and $Al_{12}Fe_3Si$ as the intermetallic materials in the alloy AA7075. They observed that the $Al_{12}Fe_3Si$ had less electrochemical function notwithstanding a nobler potential and was unable to sustain enough cathodic current that could have a significant impact on the corrosion kinetics. However, they

© 2024 The Author(s). Published by the Royal Society of Chemistry

Open Access Article. Published on 09 October 2024. Downloaded on 7/19/2025 2:17:10 AM. This article is licensed under a Creative Commons Attribution-NonCommercial 3.0 Unported Licence.

submitted that even particles that could not participate in galvanic coupling with the matrix were still prone to crevice and intergranular corrosion. Studies have shown that there is a link between the electrochemical behaviors of some IMPs and the pH of the solution.[92–94] Thus, even though Al(Fe, Mn, Cr)Si and Al_3Fe compounds are both net cathodic sites in an alkaline solution, both particles continue to undergo anodic oxidation, which alters their composition and morphology, affecting their cathodic reactivity.[94] Al_3Fe intermetallic particles precipitated during the annealing of binary Al–Fe alloys showed increased cathodic reactivity behavior. In addition, Al_3Fe served as a site for localized pitting.[87] Al_2CuMg (S phase) intermetallic particles which are most abundant in Al 2024-T3 and have been determined to be largely responsible for its vulnerability to localized corrosion. Where the corrosion tendency is less, the intermetallic was firstly anodically polarized within the matrix, resulting in the dissolution of Mg and release of Cu, which could be oxidized to produce ions on the exterior surface. The enriched Cu residue acted as a cathode, promoting swift oxygen reduction leading to the corrosion process in the structure.[94–96] In another study by Zhu *et al.*[97] Si particle acted as a cathodic part while, Mg_2Si was anodic, and corrosion occurred within the surface at the initial time. Notwithstanding, the Mg_2Si compound transformed from anode to cathode during the corrosion process as a result of the dissolution of Mg and the build-up of Si. Furthermore, this transition led to the anodic dissolution of the substrate close to its edges.

6 Galvanic corrosion evaluation (electrochemical behavior of intermetallic phases in the context of aluminum alloys)

This section presents a survey regarding the electrochemical characteristics of intermetallic distinct phases commonly present within aluminum (Al)-based materials. These beneficial mechanical characteristics of several well-known aluminum materials were attributed to the heterogenous microstructures, which include intermetallic phases, enhanced *via* meticulous alloying inputs with heat treatment. However, from a localized corrosion perspective, these commonly distributed intermetallic phases would show electrochemical properties that vary with the alloy's structure, because of their richness in specific alloying elements. Consequently, this renders the alloy to be prone to several types of corrosion.[1–3] Likewise, some studies showed the evaluation of the outcome of these intermetallic phases on the corrosion behavior of Al materials. According to Birbilis and Bucheit,[3] these intermetallic phases are precursors for pitting type corrosion. They pointed out from their study that contrary to the known ideology in most metals/alloys that pitting initiation arises from the deterioration of material surface,[3–8] pitting within Al alloys was highly affected in the intermetallic phases, thus exhibiting unique surface material features, as compared to the structure. Based on this phenomenon, localized galvanic corrosion may occur where the intermetallic may act either as anode or cathode based on the elemental composition and its reactivity, as will be discussed next.

Previously, Liao and Wei[9] carried out a study on galvanically coupled Al to different part model materials (Al–Fe–Cu–Mn and Al–Fe alloys) to simulate the intermetallic component usually found in Al alloys. Their findings revealed that a significant galvanic current existed within Al and the studied alloys, which suggests that galvanic coupling can aggravate the corrosion of the couples investigated. Furthermore, Birbilis and Bucheit[3] attempted in their study to classify intermetallic in 7*xxx* series Al alloy according to their electrochemical activity. According to their study, the first category of intermetallic in the studied alloy is the noble intermetallic having increased electrochemical functions like Al_7Cu_2Fe and Al_2Cu. These alloys could sustain large cathodic current, and as such are possibly associated with peripheral pitting arising from the galvanic corrosion with the alloy's matrix. The second category is the noble particle with low electrochemical activity, for example, Al_3Zn. This category of intermetallic does not sustain large cathodic currents, and as such cannot adversely impact the corrosion kinetics of the alloys. Hence, pitting is not often associated with this intermetallic type. Thirdly, is the active intermetallic phase with high self-dissolution rates such as $MgZn_2$. This type can undergo anodic dissolution at high rates. Finally, the last category is the active intermetallic phase with noble element components, for example, Al_2CuMg. This type may undergo dealloying and incongruent dissolution, thereby leading to polarity reversal. Also, this type can be selectively dissolved giving rise to peripheral pitting. Moreover, they pointed out that the characteristic values of corrosion potential for intermetallic phases are dependent upon their chemical composition. Intermetallics containing Cu, Fe, and Ti are observed to be more noble than pure Al or its matrix. Such intermetallics, which include Al_3Fe, Al_7Cu_2Fe, Al_2Cu, and Al_3Ti revealed a characteristic breakdown potential in their findings, and as such, indicate that they can maintain a passive film. In contrast, intermetallics consisting of Mg, Zn, or Si are typically less noble than pure Al or its containing matrix alloy. These intermetallics such as $Al_{32}Zn_{49}$, $MgZn_2$, and Mg_2Si do not show any breakdown potential and are capable of corroding freely above their corrosion potential.

7 Electrochemical/galvanic corrosion behavior of selected/important intermetallic compounds in aluminum alloy

7.1 The Q-phase ($Al_4Cu_2Mg_7Si_8$)

Unlike the regular susceptible carbon steel that is applied in corrosion studies,[98,99] the aluminum alloy shows a prominent second phases during the corrosion process, an example is the Q-phase ($Al_4Cu_2Mg_7Si_8$).[100,101] The mechanisms of corrosion of the Q-phase in Al alloy were reported in some recent literature. According to Fleming *et al.*,[101] the aluminum with the Q phase was exposed to different experimental procedures; the mixed, braze, and heat zones procedures. These were modeled by adopting thermochemical simulations and characterized experimentally.

Open Access Article. Published on 09 October 2024. Downloaded on 7/19/2025 2:17:10 AM.
This article is licensed under a Creative Commons Attribution-NonCommercial 3.0 Unported Licence.

The corrosion results showed that each zone had its unique corrosion surface morphology that is linked with the chemical constituents and metallurgical features. Notably, the AA6061 and the Al–Si braze combine favored the increased intergranular corrosion mechanism within the Si-rich region leading to grain boundary β and Q ($Al_4Cu_2Mg_8Si_7$) phases, in addition to

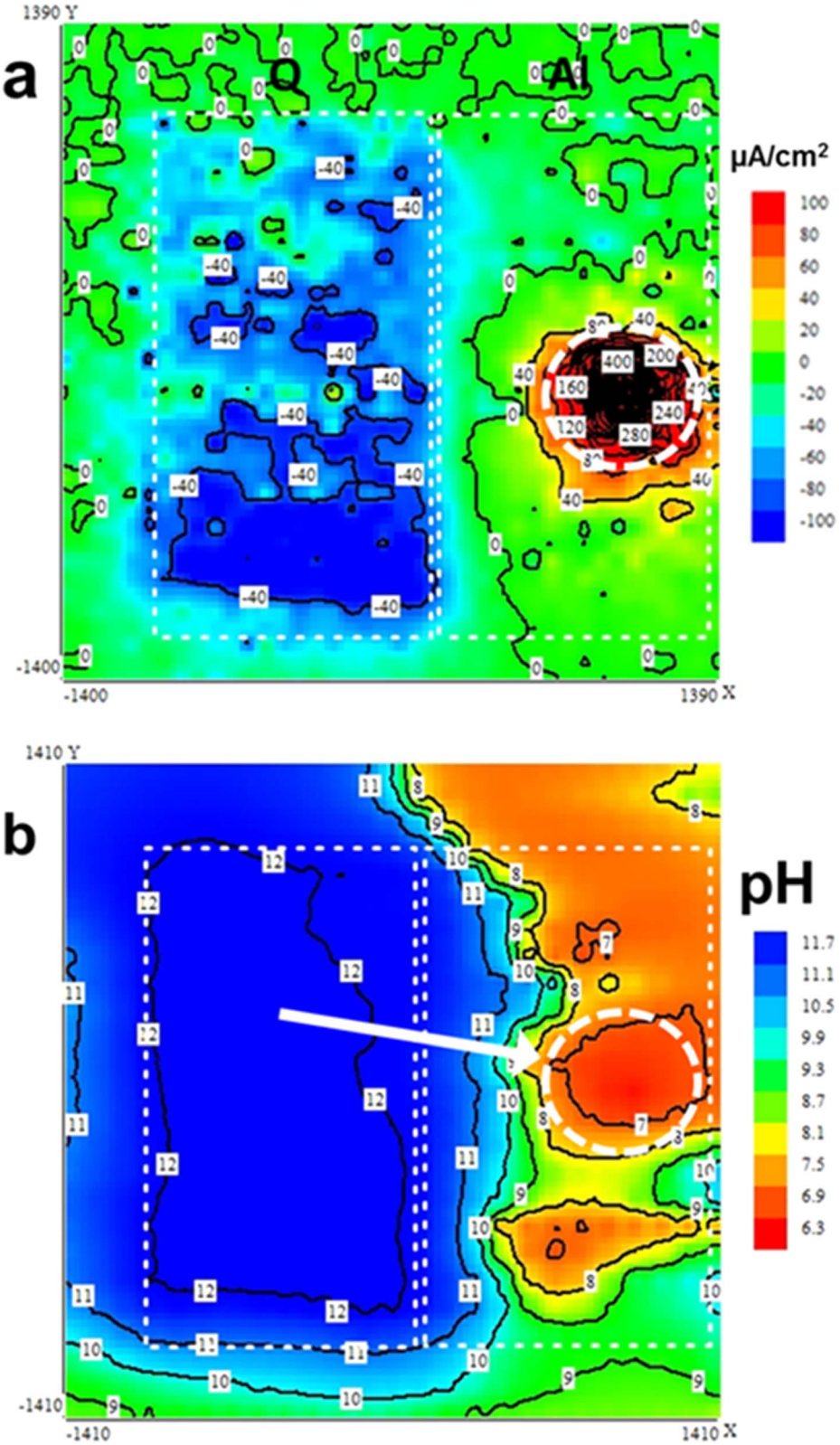

Fig. 9 Successive SIET-SVET scan of the Q-phase/Al couple after an hour in NaCl containing solution at 6 pH value: (a) SVET current density map, and (b) SIET pH map. This figure has been adapted/reproduced from (ref. 8) with permission from ELSEVIER, copyright 2024.

© 2024 The Author(s). Published by the Royal Society of Chemistry

Open Access Article. Published on 09 October 2024. Downloaded on 7/19/2025 2:17:10 AM. This article is licensed under a Creative Commons Attribution-NonCommercial 3.0 Unported Licence.

eutectically produced Si components at solidification boundaries. The pitting corrosion occurred in the NaCl media as confirmed by the cathodic and anodic polarization measurements. These data showed that micro galvanic coupling betwixt grain boundary Q and possibly Mg_2Si compared to the Al–Cu–Mg alloy component and eutectically produced Si.[101]

In a detailed investigation by Ikeuba and co-workers[8,102] on the bimetallic corrosion of the Q-phase/Al couple in solutions containing NaCl applying SVET, SIET, and EDX techniques, it was found that the galvanic corrosion of the couple is dependent on pH and immersion time. SVET images reveal that the cathodic and anodic processes emerge from Q-phase and Al, respectively under all pH environments, indicating that the galvanic polarity of the Q-phase does not depend on the pH. The galvanic effect was more pronounced in acidic and basic mediums. The SIET pH result proves that the galvanic actions of the Q-phase/Al couple progress through heavy alkalization of the surface of the Q-phase with the formation of a substantial amount of OH^-. Worthy to note is the concordance between the SVET and SIET maps. Fig. 9 is a successive SIET-SVET scan of the Q-phase/Al couple after an hour in NaCl solution at pH 6. The Cu enrichment as observed by EDX is liable for the cathodic actions of the Q-phase in the Q-phase/Al couple. Localized anodic regions were seen on the Al surface while a uniformly distributed cathodic region was noted on the Q-phase. Worthy to note is the high degree of consistency of SVET and SIET maps which indicates that significant amounts of OH^- ion (Fig. 9b) are formed by the cathodic reactions (Fig. 9a) on the Q-phase surface. An exceptionally low pH region is observed in Fig. 9b shown by the white circular disconnected lines. This low pH area corresponds in sense and magnitude sense to the area of high anodic activity on Al in the SVET map.

Similarly, in further experiment that was conducted in NaCl media within various pH adopting cathodic and anodic potentiodynamic polarization, time-of-flight secondary ion mass spectroscopy (ToF-SIMS), and X-ray photoelectron spectroscopy (XPS) presented a corrosion characteristic of the Q-phase ($Al_4Cu_2Mg_8Si_7$).[103] The potentiodynamic polarization curves show that the corrosion mechanism of the Q-phase was dependent on pH and encourages fast anodic and cathodic reaction kinetics within the alkaline and acidic media. The corrosion potentials ranged between 0.5–1.3 V_{SCE} from the acidic to the basic region. The order of the corrosion process rate was pH 6 < pH 4 < pH < 10 < pH 2 < pH 12 pH < 13 < pH 1. The surface morphology data showed that the dissolution of prominent elements like Al, Mg, and Si occurred amid the corrosion of the Q-phase promoting Cu-rich rubbles independently spread within the neutral area and evenly dispersed in the alkaline area.[104–107]

7.2 The π-phase ($Al_8Mg_3FeSi_6$)

The π-phase is one of the unique intermetallics found in aluminum–Si based alloys.[103,104] The basic behavior of Al–Si based alloys are influenced by the presence of impurity components especially at the point of casting and melting. The impurity often produces intermetallic elements with diverse sizes, types, morphology, and its concentration depends mostly on the alloying composition, thermal history, cooling tendency, and many other factors. The presence of these compounds, especially with varying morphology and size, tends to be the cause ascribed for the relative effects of localized corrosion that take place on metals. The typical examples of these intermetallic compounds are α-$Al_{15}Fe_3Si_2$, β-AI_5FeSi, and π-$Al_8M_3FeSi_6$.[104]

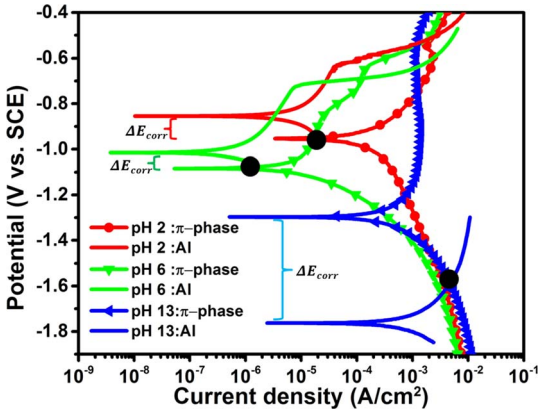

Fig. 10 The π-phase and pure Al potentiodynamic polarization plots in sodium chloride solutions at different pH values. This figure has been adapted/reproduced from (ref. 103) with permission from Elsevier, copyright 2024.

In a recent report by Ikeuba *et al.*,[103] the bimetallic corrosion of π-$Al_8Mg_3FeSi_6$ phase and pure Al in different media (acidic, neutral, and basic solutions) was investigated with respect to time and pH using potentiodynamic polarization, SVET and EDX. Polarization results revealed that the π-phase show distinct corrosion potentials ranging from −0.8 to −1.3 V_{SCE} from the acidic to the basic environments. The π-phase was noted to dissolve actively both in acidic and basic environments with high current densities. The galvanic behaviour of the of the π-phase with respect to Al was also revealed by polarization tests. It was revealed (Fig. 10) that in acidic and near-neutral environments, the π-phase acted as the anode while Al acted as the cathode, although the opposite was seen under basic environments. SVET current density maps revealed that in acidic and basic environments, the anodic and cathodic sites develop from the π-phase and Al, respectively. While under neutral conditions, self-dissolution of π-phase happens and both anodic and cathodic activities emerged from the π-phase with no significant activity on Al. The intensity of the galvanic corrosion was more pronounced in acidic and basic solutions, and the rank of the intensity of the galvanic effect is pH 13 > pH 2 > pH 6. EDX revealed the selective release of more electropositive elements in the π-$Al_8Mg_3FeSi_6$ phase leading to the enrichment of less active elements which in turn impacts the galvanic polarity of the π-$Al_8Mg_3FeSi_6$.

According to MÖLler *et al.*, 2010, the tensile and microstructure characteristics of some solid substrate alloys having low to high concentrations of Cr, Ni, and Fe undergo different temperature conditions. The detailed influence of most of the intermetallics on tensile characteristics that is obtainable in

Open Access Article. Published on 09 October 2024. Downloaded on 7/19/2025 2:17:10 AM.
This article is licensed under a Creative Commons Attribution-NonCommercial 3.0 Unported Licence.

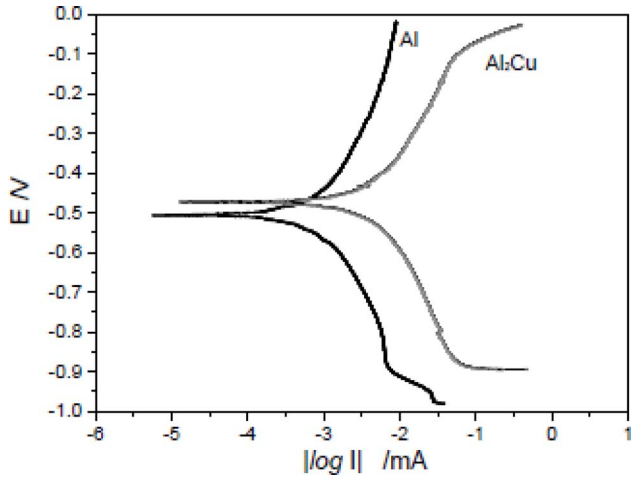

Fig. 11 Potentiodynamic polarization plots for Al_2Cu and pure Al in 0.1 M Na_2SO_4 solution. This figure has been adapted/reproduced from (ref. 108) with permission from Elsevier, copyright 2024.

corrosion processes was analyzed. The data obtained from the study indicates high concentrations of Cr, Ni, and Fe. The results are linked with the production of many π-$Al_8FeMg_3Si_6$ phases, which get rid of strengthening Mg atoms out of the solid solution. In addition, the ductility recorded for large concentrations of Cr, Ni, and Fe levels alloy was shown to decrease noticeably because of the corrosion microcracking of the higher volume ratio of Al_9FeNi and π-$Al_8FeMg_3Si_6$ phases.[107]

7.3 The θ-phase (Al_2Cu)

Al_2Cu is a significant intermetallic compound that has a huge impact on the A1-alloy corrosion behavior. Due to the intermetallic Al_2Cu's small size, it is grievously challenging to continually examine corrosion behavior and its mechanism for bulk Al alloy. The coarse Al_2Cu crystallite has been reported to have a significant impact on the 2024 alloy's cathodic process which was also connected to the sensitivity to pitting. Zhou *et al.*[108] argued that for local and microscopic corrosion of 2024 alloy, the Al_2Cu phase was crucial. They went further to state that the choosy dissolution of Al in the θ-phase (Al_2Cu) produced a penetrable copper-rich residue as well as the θ-phase's de-alloying. Because of the nearby low pH environment, the de-alloying in the phase could occur preferentially below the sample surface. In materials with an Al–Cu complex structure, the Al_2Cu phase has been discovered to be the cause of corrosion and a catalyst for corrosion, with the Cu concentration having no impact on the open circuit potential.[108]

Zhou *et al.*[108] reported the potential of intermetallic Al_2Cu in 0.1 M Na_2SO_4 to be −473.04 mV, which is comparable to the potential in a 0.5 M H_2SO_4 solution.[109,110] According to the prior finding mentioned in the literature, the potential of pure Al is more negative than that of intermetallic Al_2Cu. This aligns with the work of Zhou *et al.*,[108] where Al was more readily dissolved in 0.1 M Na_2SO_4 than intermetallic Al_2Cu as shown in Fig. 11. They further revealed that thick and uneven corrosion product in the local areas which is attributed to the accumulation of the corrosion product. Pitting corrosion was more noticeable in the Al region than intermetallic Al_2Cu as displayed in Fig. 12. They concluded that linked Al_2Cu/Al has galvanic corrosion, which results in pure Al being easily dissolved and acting as the anode while intermetallic Al_2Cu is shielded and acting as the cathode.

Also, the galvanic corrosion study of alloys of aluminum–copper model containing α- and θ-phases in 0.1 M Na_2SO_4 by Idrac *et al.*,[111] revealed that the cathodic θ-phase is more prone to pitting caused by sulfate ions. When there is a greater disparity between the copper contents of the anode and the cathode, the cathode's θ-phase is more sensitive to pitting. The sensitivity to pitting in sulfate solutions by any phase increases in direct proportion to the copper content.

Immersion of intermetallic Al_2Cu in an acidic solution of 0.1 M Na_2SO_4 that mimics an atmosphere polluted by industry, the principal effects that happen are oxygen reduction at the cathode and the anodic dissolution of Al. The dissolution reactions are given as:[112]

$$Al - 3e \rightarrow Al^{3+} \quad (1)$$

$$O_2 + 4H^+ + 4e^- \rightarrow 2H_2O \quad (2)$$

Due to the mild acid environment, the following reactions took place concurrently:

$$H_2O + \rightarrow H^+ + OH^- \quad (3)$$

$$Al^{3+} + 3OH^- \rightarrow Al(OH)_3 \quad (4)$$

$$Al(OH)_3 \rightarrow AlOOH + H_2O \text{ or } 2Al(OH)_3 \rightarrow Al_2O_3 + 3H_2O \quad (5)$$

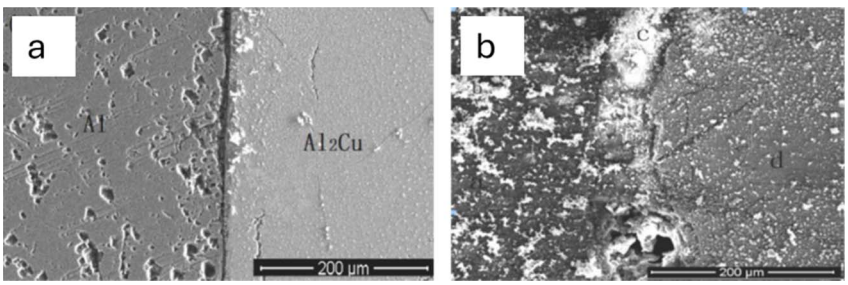

Fig. 12 Surface morphology of Al_2Cu/Al surface picture without and after immersion (a) 0 h; (b) 96 h of 0.1 M Na_2SO_4. This figure has been adapted/reproduced from (ref. 108) with permission from Elsevier, copyright 2024.

© 2024 The Author(s). Published by the Royal Society of Chemistry

Open Access Article. Published on 09 October 2024. Downloaded on 7/19/2025 2:17:10 AM.
This article is licensed under a Creative Commons Attribution-NonCommercial 3.0 Unported Licence.

$$Al_2O_3 + 6H^+ \rightarrow 2Al^{3+} + 3H_2O \quad (6)$$

$$2Al^{3+} + 3SO_4^{2-} + xH_2O \rightarrow Al_2(SO_4)_2 \cdot xH_2O \quad (7)$$

The intermetallic Al_2Cu or linked Al_2Cu/Al sample surface's corrosion behavior may be explained by these processes. Al and Al's oxide dissolve during the first stage of immersion when intermetallic Al_2Cu or linked Al_2Cu/Al is submerged in the solution. Both the dissolution and formation of the Al oxide occur simultaneously. The primary effect of the hydrogen ions being consumed is the formation of Al oxide. Al oxide, which shields the surface of the sample, is, therefore, the primary corrosion product. The corrosion product and mechanisms of intermetallic Al_2Cu, however, are yet unclear due to the influence of significant structural changes in the material.

7.4 The S-phase (Al_2CuMg)

Due to its superior weight–strength ratio, the 2024-T3 aluminium alloy utilizes an essential intermetallic phase called S-phase (Al_2CuMg) to increase its mechanical strength. Among the several intermetallic phases in 2024-T3, the Al_2CuMg is the most prevalent among them.[113] The addition of Cu and Mg elements in Al_2CuMg enhances its high strength. These two substances, however, have a severe negative impact on the alloy's ability to resist corrosion. Researchers are quite interested in the function that Al_2CuMg plays in the 2024-T3 aluminum alloy corrosion, thus they have put a lot of work into studying this phenomenon.[114–126]

The process of corrosion of intermetallic Al_2CuMg ingrained in an aluminum matrix is traditionally studied to figure out the corrosion mechanism of these intermetallic particles. This technique provides in-depth knowledge of the chemical and electrochemical mechanisms involved when corrosion forms on an alloy's surface. This method's drawback is that it is challenging to identify chemical species and electrochemical behavior at the edges of particles and the bottom of pits due to continuing erosion. Despite some consensus regarding the corrosion of Al_2CuMg, there are disagreements regarding its role in the corrosion of the enclosing Al matrix. The argument is that the pitting of the Al matrix phase also takes place at the

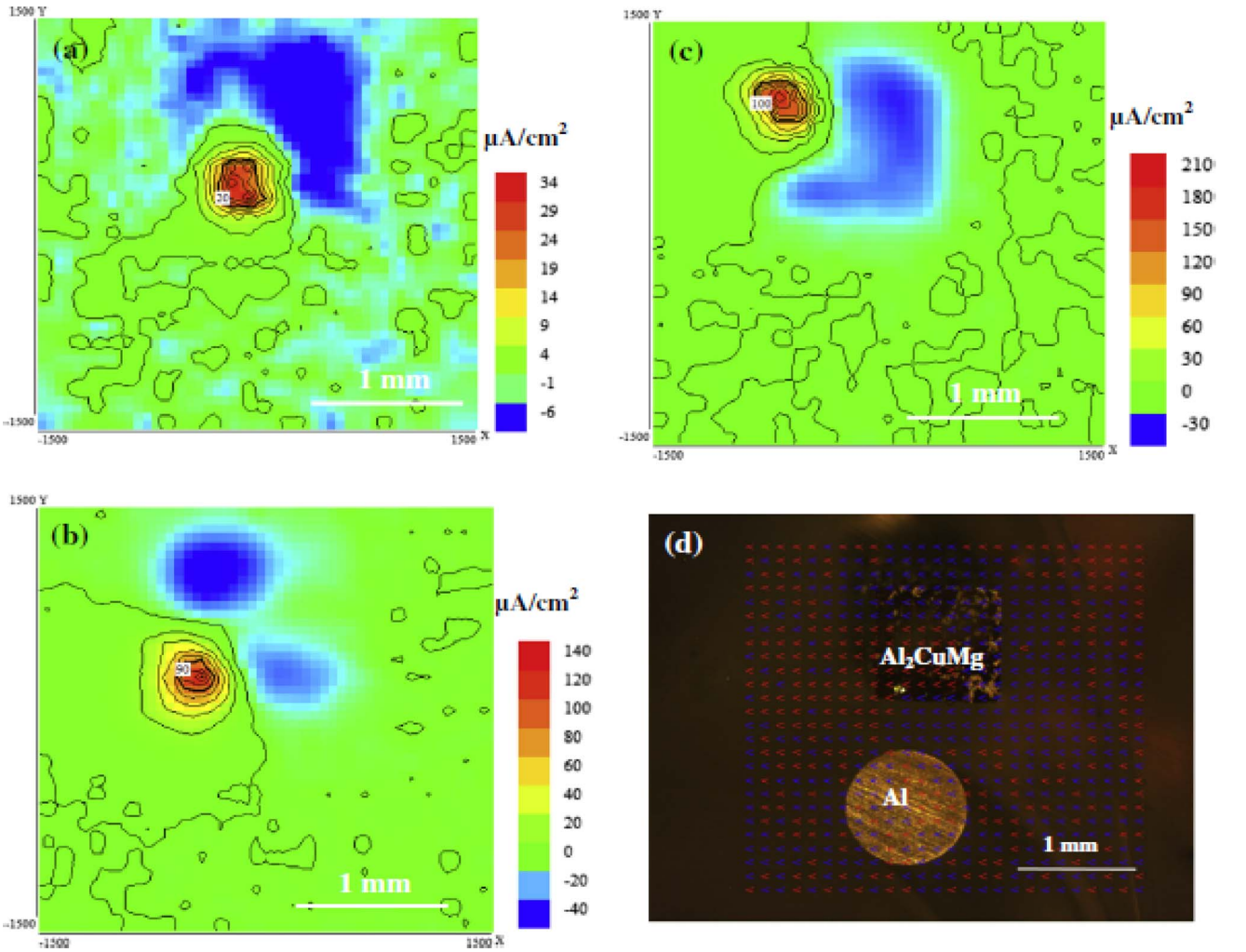

Fig. 13 Al_2CuMg–Al coupling current density map after (a) 1 h, (b) 4 h, and (c) 24 h of immersion in 0.005 M NaCl, (d) optical image after exposure for 24 h.[113] This figure has been adapted/reproduced from (ref. 113) with permission from Elsevier, copyright 2024.

Open Access Article. Published on 09 October 2024. Downloaded on 7/19/2025 2:17:10 AM. This article is licensed under a Creative Commons Attribution-NonCommercial 3.0 Unported Licence.

edges of particles of intermetallic Al_2CuMg, even though prepared Al_2CuMg has open-circuit potentials (OCP) of 0.920 to 0.930 V, which are 0.300–0.400 V lower than the OCP of 2024-T3.[127,128] X-ray line scans through Al_2CuMg particles were used to detect the dealloying of Mg and Al from Al_2CuMg particles. Their research also revealed that the Al content of the Al_2CuMg particles had decreased. In the exceedingly early stages of immersion, it was also discovered that the Al matrix around Al_2CuMg particles was heavily dissolving, and that Mg and Al had been dealloyed from the Al_2CuMg particles.[127] According to Zhu *et al.*[118] the disintegration of the Al matrix was significantly more severe early on than it was later. The localized alkalization brought on by the associated cathodic reaction was assumed to be the cause of the Al dissolution. According to other researchers,[128] Mg and Al dealloyed from the S phase, and the Al matrix trenched when submerged in a NaCl solution. Most of the aforementioned studies stated that the difference in potential between the Al_2CuMg and the Al matrix encourages anodic dissolution, whereas the Cu-enriched residue operates cathodically and stimulates the disintegration of the Al matrix at the nearby boundary of Al_2CuMg precipitates.[120,128] Zhu *et al.*,[118] on the other hand, concentrated on the significance of Al matrix dissolution because of local alkalization. There is debate over the electrochemical nature of Al_2CuMg which contradicts the anodic property during the preliminary stages of immersion. When scientists examined their Volta potentials, it was evident that Al_2CuMg particles were more cathodic than the alloy matrix. Specifically, the S phase was discovered by atomic force microscopy (AFM) scanning potential to be nobler than the Al matrix surrounding it.[129–132]

In SIET currents, chloride concentration, and pH measurement of Al_2CuMg in a simulated corrosion environment by Shi *et al.*,[113] Al_2CuMg exhibited both anodic and cathodic reactions, whereas Al exhibited neither of these behaviors. With more time spent submerged, the maximum anodic currents rise. According to the distribution of current density, self-dissolution rather than anodic reaction caused by coupling with Al_2CuMg was the source of the alloy's dealloying as shown in Fig. 12. After being submerged for 24 hours, Al_2CuMg's corrosion products may be seen on the material's surface.

After 1 hour of immersion, the Al_2CuMg–Al coupling's pH map (Fig. 13) revealed that the pH levels at the anodic and cathodic sites were both in the alkaline region (8–10.8 pH range) caused by the abundance of hydroxyl ion produced when Al_2CuMg self-dissolved. There was no evidence of an acidic area.

A change in pH can cause chemical disintegration, which in turn can cause the Al matrix to corrode. The Al oxide layer and Al matrix will dissolve chemically actively if pH surpasses 9:

$$Al_2O_3 + 2OH^-(ad) \rightarrow 2AlO_2^-(ad) + H_2O \quad (8)$$

$$2Al(m) + 3H_2O \rightarrow Al_2O_3(ad) + 3H_2 \quad (9)$$

As a result, it may be assumed that Al_2CuMg's self-dissolution can cause the Al matrix to trench around it. The following succinctly describes the anodic and cathodic reactions on the Al_2CuMg:[133]

$$Mg + 2H_2O \rightarrow Mg^{2+} + 2OH^- + H_2 \quad (10)$$

$$2Al + 6H_2O \rightarrow Al^{3+} + 6OH^- + 3H_2 \quad (11)$$

$$Mg \rightarrow Mg^{2+} + 2e \quad (12)$$

$$Al \rightarrow Al^{3+} + 3e \quad (13)$$

$$O_2 + 2H_2O + 4e \rightarrow 4OH^- \quad (14)$$

7.5 Al_3Mg_2 intermetallic compounds

Al_3Mg_2 (β-phase) intermetallic compounds usually form active precipitate at the grain boundary of aluminium 5000 series alloys when exposed for a long time at 50–200 °C temperatures in a process commonly referred to as "Sensitization".[134,135] Both the sensitization process and corrosion performance have been reported to rely on the thermomechanical process, the composition of the alloy, and the sensitization temperature. Although

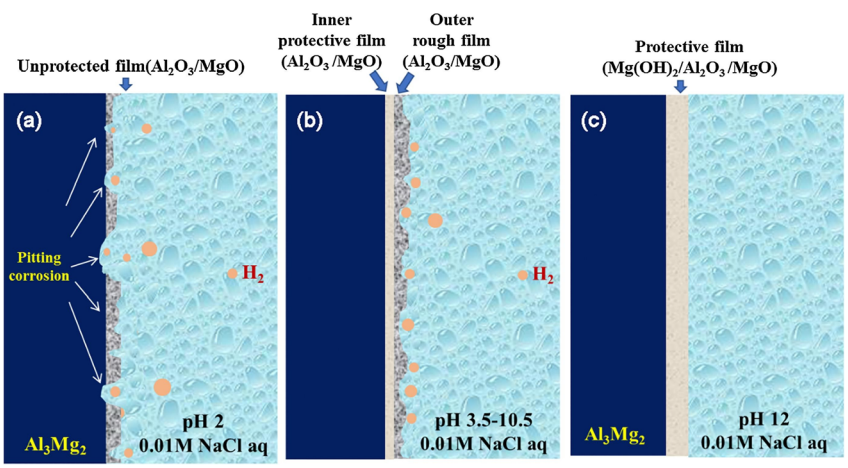

Fig. 14 The schematic of the surface physical models of Al_3Mg_2 after immersion in 0.01 M NaCl solution of (a) pH 2; (b) pH 3.5–10.5 and (c) pH 12.[139]

© 2024 The Author(s). Published by the Royal Society of Chemistry

Open Access Article. Published on 09 October 2024. Downloaded on 7/19/2025 2:17:10 AM.
This article is licensed under a Creative Commons Attribution-NonCommercial 3.0 Unported Licence.

β-phase precipitation does not have a huge influence on the mechanical properties of the alloy because it is not a hardening precipitate,[136] however, β-phase can affect the stress corrosion cracking (SCC) or intergranular corrosion (IGC) susceptibleness in seawater or other corrosive environments.[137] Electrochemistry of β-phase has been reported to be anodic with reference to an Al-based matrix, with the corrosion potential being less noble when compared to the Al-alloys matrix in which they populate. Hence, the selective disintegration of the β-phase formed at grain boundaries can result in corrosion infiltrating deeply into the material without a huge weight deficit. This IGC makes the alloy very prone to SCC when undergoing tensile stress.[138]

Considering that the galvanic corrosion takes place betwixt the β-phase and the neighboring alloy matrix because of the distinction in the electrochemical activities, it becomes necessary to understand the corrosion mechanism of the Al_3Mg_2 intermetallic compound and its part in the corrosion of aluminium 5000 series alloys. In this regard, Li *et al.* investigated the influence of pH on the electrochemical behavior of β-phase Al_3Mg_2 and how it affects the corrosion of AA5000 series alloy in NaCl solution.[139] Their findings proved that bulk Al_3Mg_2 behaves as an anode at pH 2–10.5 but works as a cathode at pH 12. Their electrochemical measurements suggest that there is strong disintegration of both Al and Mg at pH 2, while selective disintegration happens at pH 3.5–12. In addition, at pH 3.5–10.5, the degree of selective dissolution of Mg element increases substantially when there is any shift from neutral pH leading to the corrosive surface having a rough outer layer and a comparatively dense inner layer as demonstrated in Fig. 14. Meanwhile, at pH 12, the selective disintegration of Al becomes prevalent and the development of compact $Mg(OH)_2$ attains complete passivity on Al_3Mg_2 surface.

Lyndon *et al.* reported that the rate of dissolution of the Al_3Mg_2 is significantly higher in alkaline mediums than in acidic mediums.[138] Using the electrochemical microcell technique, Buchheit and Birbilis proved that Al_3Mg_2 is an active phase with a potential window of passivity in NaCl

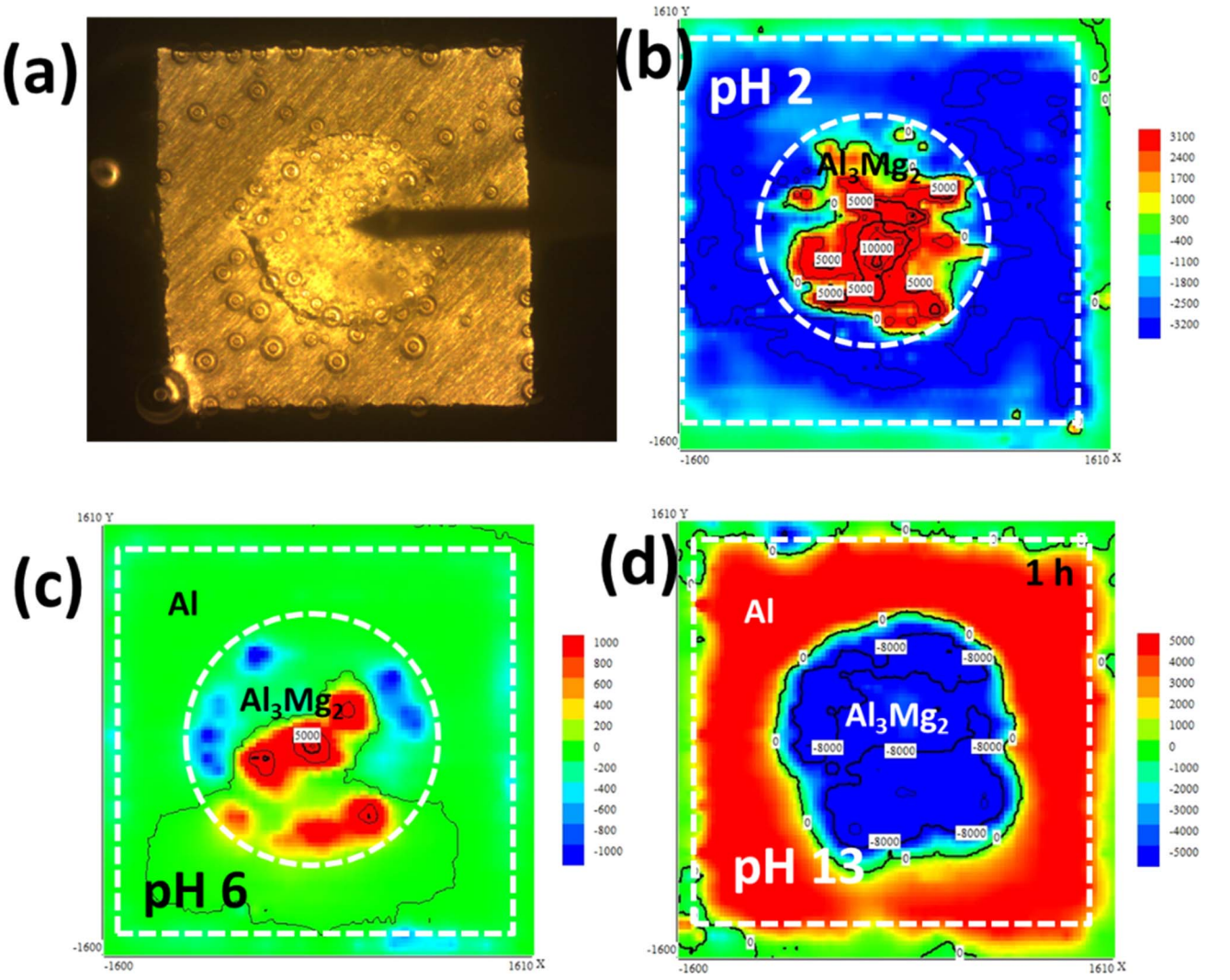

Fig. 15 SVET current density distribution on Al_3Mg_2 embedded in pure Al matrix in 0.1 M NaCl solutions at different pH values (a) microscopic image of sample-probe arrangement (b) pH 2, (c) pH 6 (d) pH 13. This figure has been adapted/reproduced from (ref. 142) with permission from IOP SCIENCE, copyright 2024.

Open Access Article. Published on 09 October 2024. Downloaded on 7/19/2025 2:17:10 AM. This article is licensed under a Creative Commons Attribution-NonCommercial 3.0 Unported Licence.

solutions.[140,141] Ikeuba *et al.*[142] made a galvanic couple consisting of Al_3Mg_2 embedded in an Al matrix to study the corrosion behavior of the β-phase (Al_3Mg_2) using SVET and ToF-SIMS. The corrosion potential was noted not to vary significantly but ranged between 1.4–1.6 V_{SCE} across the acidic to the basic environment. Their findings further confirmed that environmental pH and exposure duration significantly affect the galvanic corrosion of the Al_3Mg_2/Al couple in aqueous solutions. The result from their SVET current density distribution maps suggests that anodic processes develop from Al_3Mg_2 at pH 2, while the cathodic processes develop from Al. Both anodic and cathodic processes are observed to develop from Al_3Mg_2 at pH 6 and 10, and there was no obvious electrochemical process on Al. The cathodic activities develop from Al_3Mg_2 at pH 13, while the anodic process develops from the Al (Fig. 15). From their ToF-SIMS results, the dealloying of Al_3Mg_2 in the galvanic couple was shown to be by selective disintegration of Mg resulting in the deposition of corrosion products populated with Mg compounds in an acidic and neutral environment. A comparably thin hydroxide-rich film was shown to form in an alkaline environment.

7.6 Mg_2Si intermetallic compound

Al–Mg–Si alloys are the commonly used high-strength Al alloys and mainly consist of Mg_2Si nanosized dispersoids as the strengthening phase.[10] The intergranular corrosion (IGC) of Al–Mg–Si alloys is affected by the composition of grain boundaries and the micro-galvanic coupling between Mg_2Si precipitates and Mg, Si segregation at grain boundaries, and precipitate-free zone (PFZ) at grain boundaries.[143] Buchheit and Birbilis performed potentiodynamic polarization tests, which showed that the corrosion potential of Mg_2Si was much lower than that of the alloy matrix.[7] The volta potential of Mg_2Si particle measured by scanning kelvin probe force microscopy (SKPFM) is about 100–180 mV smaller than that of the Al matrix,[144] indicating that the Mg_2Si particle was initially anodic with respect to the Al matrix. He *et al.*[143] also confirmed that Mg_2Si phases were anodic with respect to the Al-based matrix and dissolved preferentially without actually influencing the propagation of the corrosion process. Gupta *et al.*[145] revealed that Mg_2Si is either a local anode or a local cathode; they found that Mg_2Si is anodic to 6360 and 7075 Al alloys in the acidic and neutral pH, but cathodic in alkaline conditions (where Al dissolves and Mg is passive). Gharbi *et al.* also proved that Mg_2Si particles can selectively dissolve in a neutral solution.[146] Employing the hydrogen evolution approach and tailored polarization schemes, Ikeuba *et al.* showed that anodic hydrogen evolution (AHE) is not very significant on Mg_2Si (β-phase).[14] Researchers have reported Selective dissolution of Mg during the corrosion of Mg_2Si phases. Fabian *et al.*[147] confirmed that MgSi particles are selectively de-alloyed by Mg in 1 M NaCl solution in a process that began within the first few seconds and stopped after about 20 min. The Si-rich Mg_2Si remnant is cathodic-active after de-alloying. Concerning the anodic activity, they show that Mg_2Si remnants do not alter the pitting potential in electrochemical micro/macro-cell experiments.

Zeng and co-workers also confirm the existence of Mg_2Si precipitates and coarse Si particles along the grain boundary of Al–Mg–Si alloys with a mole ratio of Mg to Si > 1.73.[148] Corrosion begins on the Mg_2Si surface and the PFZ on the adjacent periphery of the Si particle. Si particles induce severe anodic dissolution and corrosion of the PFZ at its adjacent periphery at prolonged corrosion time. In addition, the Si particles increase the rate of preferential dissolution of Mg in Mg_2Si precipitate, accelerating the polarity transformation between Mg_2Si and the PFZ, hence, the corrosion of the PFZ at the adjacent periphery of Mg_2Si precipitate is improved. Li *et al.*[149] investigated the galvanic corrosion behavior of β-phase (Mg_2Si) in NaCl solution *via* SVET confirming that the Mg_2Si intermetallic compound dissolves in acidic and near-neutral solutions but passivates in alkaline solution. The passivation was ascribed to the formation of $Mg(OH)_2$ and MgO films on the Mg_2Si surface which prevents it from further dissolution. They proved that the dealloying of binary Mg_2Si phase is dependent on the pH of the solution and corrosion time where an increase in the pH decreases the corrosion rate. Wolka and co-workers determined the OCP of Mg_2Si *via* a microcapillary electrochemical cell and suggested that the acceleration of OCP after immersing 1 hour in 0.01 M NaCl solution can be attributed to the preferential dissolution of Mg.[150] Likewise, Mg_2Si particles in Al–Mg–Si alloys have been studied by employing SKPFM together with AFM, electrochemical micro-cell measurements combined with electron probe microanalysis (EPMA), and auger electron spectroscopy (AES). These studies confirmed that the high reactivity of Mg results in the dealloying of Mg_2Si particles along with the Si ennoblement enabling the Mg_2Si remnant to exhibit cathodic activity.[151,152]

7.7 The δ (Al_3Li)

7.7.1 Electrochemical potentials. A class of lightweight, high-strength materials known as aluminum–lithium alloys has attracted interest in some industrial applications, particularly in the aerospace sector.[153] Lithium has been discovered to improve the strength-to-weight ratio of the resultant alloy, as well as increase its corrosion resistance.[154] One such alloy is Al_3Li, which has a particularly low density and high specific strength.[155] Researchers have studied Al_3Li's electrochemical potentials in a variety of situations to better comprehend the material's electrochemical characteristics. Studies on Al_3Li potential, for instance, have been done in both the presence of chloride ions and acidic solutions.[156,157] Such studies have found that the electrochemical behavior of Al_3Li can vary significantly depending on the specific conditions of the environment. Due to Al_3Li's high theoretical specific capacity and low volume expansion, several researchers have investigated using it as a viable anode material in lithium-ion batteries.[158,159] However, challenges still exist in achieving stable cycling performance, particularly in terms of preventing the evolution of a solid-electrolyte interphase (SEI) layer on the surface of the electrode.[160] In general, Al_3Li electrochemical potentials represent a significant area of study with potential ramifications for a variety of industrial and technological applications. To

© 2024 The Author(s). Published by the Royal Society of Chemistry

Open Access Article. Published on 09 October 2024. Downloaded on 7/19/2025 2:17:10 AM.
This article is licensed under a Creative Commons Attribution-NonCommercial 3.0 Unported Licence.

completely comprehend how this material behaves in various settings and circumstances, however, additional research is required.

7.7.2 Pitting potentials. Aluminum–lithium alloys, and particularly Al_3Li, have been the subject of much research owing to their desirable mechanical and physical properties, such as high strength-to-weight ratio and good corrosion resistance.[160] However, the susceptibility of these alloys to localized corrosion, like pitting corrosion, has been a concern in some applications.[161] Pitting corrosion is a type of localized corrosion that poses a serious threat to a variety of industries because it can quickly and unexpectedly cause material failure. To better understand the pitting behavior of Al_3Li, researchers have studied its pitting potential in various environments. For example, studies have investigated the effect of chloride ion concentration on the pitting potentials of Al_3Li.[154] These studies have discovered that the Al_3Li's pitting potentials decrease as the concentration of chloride ions rises, suggesting that the presence of chlorides may make Al_3Li more susceptible to pitting corrosion. Other studies have explored the influence of various surface treatments on the pitting potentials of Al_3Li.[162–164] These studies have found that certain surface treatments, such as electropolishing or anodizing, can significantly increase the pitting potentials of Al_3Li, potentially improving its resistance to pitting corrosion. Overall, the pitting potentials of Al_3Li are an important area of research for understanding its corrosion behavior in different environments and for developing effective corrosion prevention strategies. To completely the factors that influence Al_3Li's tendency to form pits and to create practical strategies for reducing this tendency, more study is required.

7.7.3 Galvanic polarity. Aluminum–lithium alloys, and particularly Al_3Li, have been extensively studied owing to their unique combination of high strength, low density, and good corrosion resistance.[155] However, when using dissimilar metals in engineering applications, it is crucial to consider their galvanic behavior when in contact with other metals. When two metals that are not compatible with one another encounter an electrolyte, such as seawater, it results in galvanic corrosion. In this situation, one metal acts as the anode, and the other metal acts as the cathode, leading to the corrosion of the anode. The galvanic series ranks metals according to how likely they are to corrode in certain conditions.

Studies have investigated the galvanic behavior of Al_3Li when in contact with other metals, including aluminum alloys and copper alloys.[165–167] These studies have found that the galvanic potential of Al_3Li is more positive than that of aluminum alloys, suggesting that Al_3Li will function as the cathode in these galvanic couples. The galvanic potential of Al_3Li is also more negative than that of copper alloys, indicating that Al_3Li will function as the anode in these galvanic couples. The galvanic behavior of Al_3Li can be affected by several factors, including the nature of the electrolyte, the area ratio between the two metals, and the presence of protective coatings or inhibitors.[166] To mitigate galvanic corrosion, it is important to select materials with similar galvanic potentials or to use coatings or inhibitors to protect the anodic material.

7.7.4 Effect of chlorides. Al_3Li alloy has exceptional corrosion resistance in a variety of conditions, including air, salt water, and acidic solutions. However, the presence of chlorides can significantly affect the corrosion behavior of these alloys. Chlorides are highly corrosive due to their ability to penetrate the protective oxide layer on the surface of metals and form complex ions that accelerate corrosion.[168] The corrosion behavior of aluminum alloys can also be affected by the concentration of chlorides, other ions present, and the solution's pH. Studies have investigated the influence of chlorides on the corrosion behavior of Al_3Li in various environments. For example, Zhao *et al.*,[158] found that the addition of 3.5 wt% NaCl to a 3.5 wt% NaOH solution significantly increased the corrosion rate of Al_3Li compared to the solution without NaCl. The addition of chloride ions also led to pitting corrosion on the surface of Al_3Li. Han *et al.*,[169] studied the effect of different types of chlorides on the corrosion behavior of Al_3Li, such as Cl-, Br-, and I-. These studies found that the corrosion resistance of Al_3Li decreased in the presence of these halide ions, with Cl-having the most significant effect. It has been demonstrated that adding inhibitors, such as rare earth metals, can lessen the impact of chlorides on the corrosion behavior of Al_3Li.[165] These inhibitors form a protective layer on the surface of the alloy, which prevents the penetration of chlorides and other corrosive species.

7.7.5 Nature of surface films (in acidic, neutral, or alkaline environments). The surface films that form on aluminum–lithium alloys, including Al_3Li play a critical role in determining their corrosion resistance. These films are typically composed of aluminum oxide and hydroxide species and are strongly influenced by the pH of the surrounding environment. In acidic environments, the surface films on Al_3Li are primarily composed of amorphous aluminum oxide (Al_2O_3) and have a thickness of a few nanometers.[170] These films have exceptional acidic corrosion resistance due to their ability to self-heal and rebuild after being damaged. The surface layers on Al_3Li in neutral conditions are a mixture of amorphous and crystalline aluminum oxide and hydroxide species. These coatings have a typical thickness of several tens of nanometers and offer considerable corrosion resistance in neutral and moderately alkaline solutions. In alkaline environments, the surface films on Al_3Li are primarily composed of crystalline aluminum hydroxide ($Al(OH)_3$).[170] These films provide good corrosion resistance in strongly alkaline solutions but may be less effective in mildly alkaline or neutral solutions. The nature of the surface films on Al_3Li can also be influenced by the presence of other species in the environment, such as chloride ions. The interaction between these species and the surface films can affect their composition, thickness, and corrosion resistance properties.

Overall, the nature of the surface films on Al_3Li concerning their acidity or alkalinity is an important consideration in determining the corrosion resistance of this alloy in various environments. More in-depth research is needed to fully understand the mechanisms of surface film formation and their interactions with different environments.

Open Access Article. Published on 09 October 2024. Downloaded on 7/19/2025 2:17:10 AM.
This article is licensed under a Creative Commons Attribution-NonCommercial 3.0 Unported Licence.

7.8 The η-phase ($MgZn_2$)

7.8.1 Electrochemical potentials. Magnesium–zinc (Mg–Zn) alloys have attracted significant attention owing to their excellent properties such as low density, high specific strength, corrosion resistance, and good biocompatibility. For an understanding of Mg–Zn alloys' corrosion behavior and the development of corrosion-resistant materials, it is essential to know their electrochemical potentials. Several methods, including galvanostatic polarization, electrochemical impedance spectroscopy (EIS), and potentiodynamic polarization, have been used to examine the electrochemical potentials of Mg–Zn alloys. According to Song *et al.*,[171] The Zn content in Mg–Zn alloys has a significant impact on their electrochemical behavior, with an increase in Zn concentration leading to greater negative potential values. The researchers also noted that by lowering the cathodic reaction rate, the addition of rare earth metals to Mg–Zn alloys might increase their corrosion resistance.

Another study by Chen *et al.*,[172] investigated the influence of microstructure on the electrochemical behavior of Mg–Zn alloys. The authors found that the presence of the $MgZn_2$ phase in the microstructure resulted in a more negative potential, indicating a higher tendency towards corrosion. However, they also reported that the presence of other phases such as MgZn and $MgZn_3$ can improve the corrosion resistance of the alloy. Some scientists have also investigated the effect of surface treatment on the electrochemical behavior of Mg–Zn alloys. According to Wu *et al.*,[173] surface modification using fluoride treatment can remarkably improve the corrosion resistance of Mg–Zn alloys by forming a protective layer on the surface furthermore, the corrosion potential of the alloy shifted towards more positive values after surface treatment.

7.8.2 Pitting potentials. Pitting corrosion is a localized form of corrosion that occurs on the surface of metals, resulting in small pits or holes that can compromise the material's structural integrity. Many variables, including the alloy's composition, the presence of impurities or defects, and the surrounding environment, have an impact on the initiation and growth of pits. $MgZn_2$ is a binary alloy comprising magnesium and zinc, having a nominal 2% zinc content. The addition of zinc improves the alloy's mechanical properties, such as strength and ductility, but also increases its susceptibility to corrosion. Several studies have investigated the pitting potentials of $MgZn_2$ in different electrolytes, such as NaCl, KCl, and H_2SO_4.

Liu *et al.*,[163] pointed out that the pitting potentials of $MgZn_2$ grew with rising pH and decreased with rising chloride concentration. They attributed this behavior to the formation of protective films on the surface of $MgZn_2$ at high pH and the breakdown of these films at high chloride concentrations. Similarly, Zhang *et al.*,[174] discovered that $MgZn_2$ had larger pitting potentials in alkaline solutions than in acidic solutions, highlighting the significance of pH in preventing pitting corrosion. Temperature, dissolved oxygen, and the presence of other ions, such as sulfate and nitrate, can also have an impact on the pitting potentials of $MgZn_2$. These variables are in addition to pH and chloride concentration. For instance, Wu *et al.*,[175] reported that the pitting potentials of $MgZn_2$ decreased with increasing temperature due to accelerated corrosion kinetics. They also found that the presence of sulfate ions inhibited pitting corrosion by forming sulfate compounds on the surface of $MgZn_2$.

The pitting potentials of $MgZn_2$ are influenced by several factors, such as pH, chloride concentration, temperature, and the presence of other ions. Understanding these factors is essential in designing and optimizing the performance of $MgZn_2$ in different environments. Further research is recommended to investigate the complex interplay between these factors and their effects on the pitting corrosion of $MgZn_2$.

7.8.3 Galvanic polarity. Galvanic corrosion occurs when two metals with different electrochemical potentials come into contact in the presence of an electrolyte. The more noble metal, with a higher electrochemical potential, acts as the cathode, while the less noble metal, with a lower electrochemical potential, acts as the anode. The anode corrodes as a result of the passage of electrons caused by the potential difference between the two metals. The relative locations of magnesium and zinc in the electrochemical series affect the galvanic behavior of $MgZn_2$ with other metals. Some researchers have investigated the galvanic polarity of $MgZn_2$ with different metals, such as aluminum, steel, and copper. In studies by Ikeuba *et al.*,[176] spanning pH ranges of 2 to 12, the behavior of produced $MgZn_2$ intermetallic particles linked with Al in 0.1 M NaCl solutions was investigated. Results show that pH and exposure duration are both crucial factors in the galvanic dissolution of $MgZn_2$.

The galvanic potential of $MgZn_2$ changed towards a more negative value when in contact with copper, suggesting that $MgZn_2$ behaved as the anode, according to research by Kim *et al.*,[177] on the galvanic behavior of $MgZn_2$ in contact with copper. They attributed this behavior to the formation of a copper-rich layer on the surface of $MgZn_2$, which enhanced the galvanic corrosion of $MgZn_2$. In addition to the relative positions of magnesium and zinc in the electrochemical series, other factors that affect the galvanic polarity of $MgZn_2$ include the composition of the electrolyte, the temperature, and the surface area ratio of the two metals.[177]

7.8.4 Effects of chlorides. The corrosion of metals and alloys, especially $MgZn_2$, is known to be accelerated by chlorides, one of the most aggressive ions. The presence of chlorides can induce pitting corrosion, crevice corrosion, and stress corrosion cracking of $MgZn_2$. Some studies have investigated the effects of chlorides on the corrosion behavior of $MgZn_2$. Li *et al.*,[178] found that the inclusion of chloride ions in the environment significantly promotes the corrosion rate of $MgZn_2$. Additionally, they stated that the decomposition of $MgZn_2$ in the presence of chloride ions was aided by the formation of zinc and magnesium hydroxides. In addition to accelerating the corrosion rate, chlorides can also affect the morphology and structure of the corrosion products on the surface of $MgZn_2$. Guo *et al.*,[179] studied the effect of chloride ions on the morphology of the corrosion products on $MgZn_2$ in artificial seawater. They found that the presence of chloride ions resulted

© 2024 The Author(s). Published by the Royal Society of Chemistry

Open Access Article. Published on 09 October 2024. Downloaded on 7/19/2025 2:17:10 AM.
This article is licensed under a Creative Commons Attribution-NonCommercial 3.0 Unported Licence.

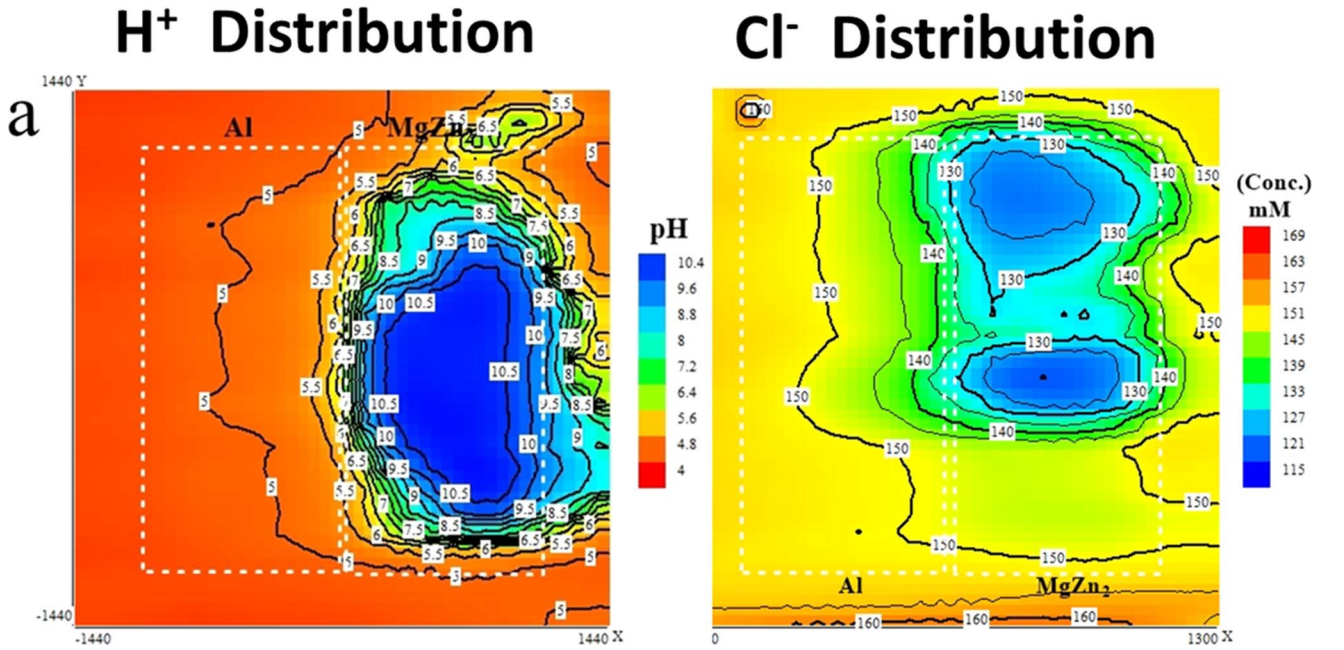

Fig. 16 (a) SIET H^+ and (b) Cl^- ion distribution map of the Al/$MgZn_2$ couple after 1 hour in 0.1 NaCl solutions at pH 4. This figure has been adapted/reproduced from (ref. 73) with permission from IOP Science, copyright 2024.

in the formation of a more porous and less compact corrosion product layer on the surface of $MgZn_2$, which further accelerated the corrosion process. This is also consistent with reports b Ikeuba *et al.*[73] which indicates low Cl-concentrations (blue region in Cl^- distribution map) in actively dissolving regions in the $MgZn_2$ which is accompanied by local alkalization (high pH blue region in Cl^- distribution map) as shown in Fig. 16.

7.8.5 Nature of surface films (in acidic, neutral, or alkaline environments). Under acidic, neutral, and alkaline circumstances, the impact of pH on the surface and interfacial films on η-phase ($MgZn_2$) in aqueous solutions has been evaluated.[180] The findings show that in an acidic environment (pH 2), substantial corrosion penetration with a dispersion of corrosion products occurred, claiming a large depth matrix cross-section. The corrosion film is seen to be stratified into two layers of different compositions under near-neutral conditions (pH 6), while in slightly alkaline conditions (pH 10) the film does not appear to be differentiated and in extremely alkaline conditions (pH 13) a compact film rich in hydroxides forms. Ikeuba *et al.*;[176] have examined how pH and applied voltage affect the electrochemical behavior of a bulk-produced $MgZn_2$ intermetallic complex in aerated 0.1 M NaCl solutions. They found that when pH increases, the anodic activity of $MgZn_2$ decreases. Furthermore, the early Mg dissolution results in a Zn-enriched surface, and the subsequent dissolution of $MgZn_2$ relies on the magnitude of the applied potential.

The corrosion behavior of $MgZn_2$ is influenced by the nature of the surface film that forms on its surface in different environments. In acidic environments, the surface film on $MgZn_2$ is primarily composed of magnesium oxide (MgO) and zinc oxide (ZnO), with small amounts of magnesium hydroxide ($Mg(OH)_2$) and zinc hydroxide ($Zn(OH)_2$) (Zhang *et al.*, 2019).[174] The cathodic reduction of dissolved oxygen and the anodic dissolution of magnesium and zinc play a major role in controlling the development of the surface layer in acidic conditions. In neutral environments, the surface film on $MgZn_2$ is primarily composed of magnesium hydroxide ($Mg(OH)_2$), with small amounts of magnesium carbonate ($MgCO_3$) and zinc carbonate ($ZnCO_3$).[31] The anodic dissolution of magnesium and zinc, as well as the chemical interaction between $Mg(OH)_2$ and CO_2, play a major role in the creation of the surface layer in neutral conditions. In alkaline environments, the surface film on $MgZn_2$ is primarily composed of magnesium hydroxide ($Mg(OH)_2$) and zinc oxide (ZnO), with small amounts of magnesium carbonate ($MgCO_3$) and zinc hydroxide ($Zn(OH)_2$) (Wu *et al.*, 2020).[173] The formation of the surface film in alkaline environments is primarily controlled by the anodic dissolution of Mg and Zn and the cathodic reduction of dissolved oxygen. The corrosion resistance of $MgZn_2$ depends on the type of surface coating that forms on it in various situations. Due to the development of a thick and protective $Mg(OH)_2$ coating, the surface film in neutral and alkaline environments, for instance, offers superior corrosion resistance than the surface film in acidic environments.[181,182]

8 The phenomenon of galvanic polarity reversal and self-dissolution

This is an important phenomenon that occurs in intermetallic compounds that are found in aluminum-based alloys given the high sensitivity of aluminum corrosion to pH changes especially when in contact with magnesium-containing intermetallic. Reports by Ikeuba and co-workers visualized the local electrochemical processes occurring in a given galvanic couple in different pH environments; this was achieved using the SVET.

Open Access Article. Published on 09 October 2024. Downloaded on 7/19/2025 2:17:10 AM.
This article is licensed under a Creative Commons Attribution-NonCommercial 3.0 Unported Licence.

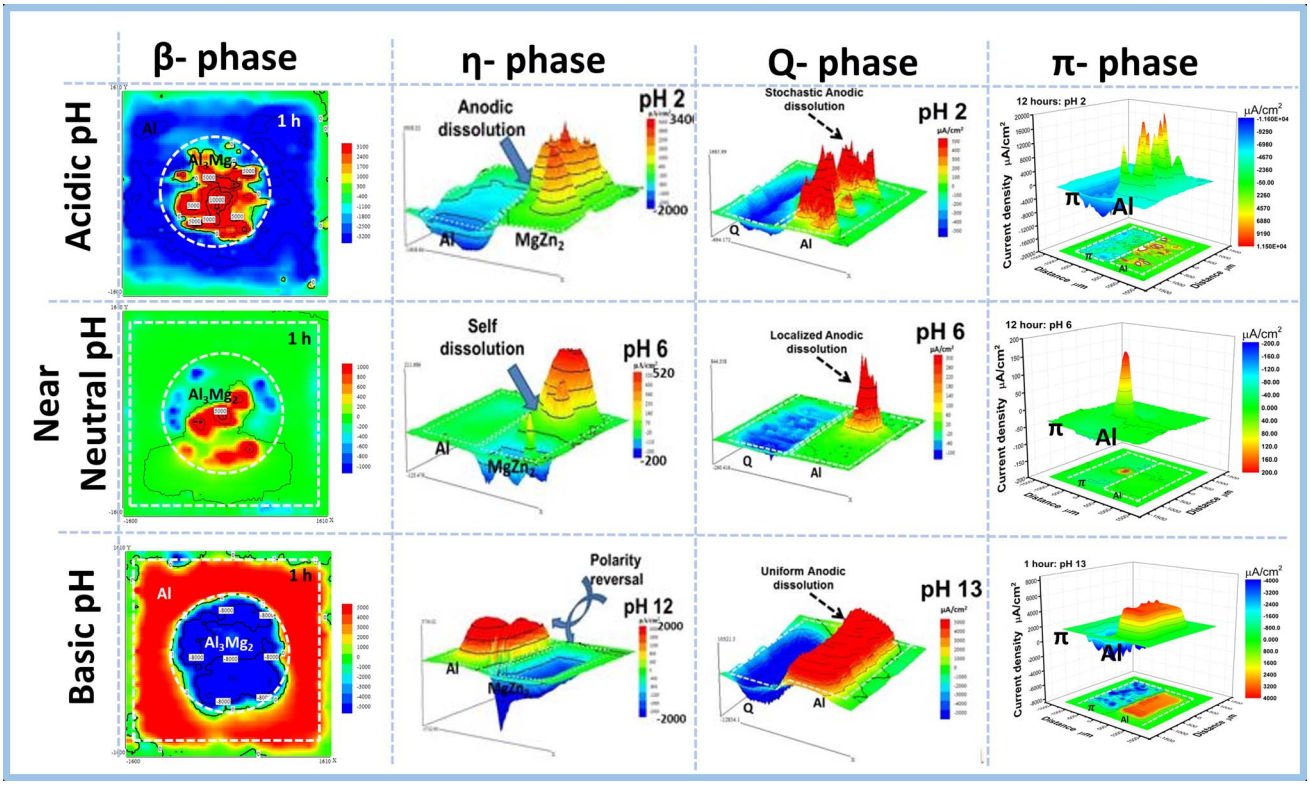

Fig. 17 SVET current density map on typical η-phase ($MgZn_2$), β-phase (Al_3Mg_2), Q-phase ($Al_4Cu_2Mg_8Si_7$), and π-phase ($Al_8Mg_3FeSi_6$) coupled to aluminum in different pH environments. This figure has been adapted/reproduced from (ref. 8, 73, 103, 131 and 142) with permission from Elsevier, copyright 2024.

Fig. 17 is a compilation of SVET current density distribution on typical η-phase ($MgZn_2$), β-phase (Al_3Mg_2), Q-phase ($Al_4Cu_2Mg_8Si_7$), and π-phase ($Al_8Mg_3FeSi_6$) coupled to aluminum in different pH environments. In Fig. 17 the red, blue, and green portions of the maps represent the acidic, basic, and neutral pH environments. The intensity of the red and blue colors represents the magnitude of the electrochemical activity occurring on the galvanic couple surface. For the β-phase (Al_3Mg_2), a 2-D current density map is presented while for the other phases, 3-D-current density maps are provided. Worthy to note is the galvanic polarity of the intermetallic phases in each environment. For β-phase (Al_3Mg_2) and η-phase ($MgZn_2$), there is a switch in the polarity of the intermetallic particles from being anodic in an acidic medium to being cathodic in a basic medium. On the other hand, the galvanic polarity of the Q-phase ($Al_4Cu_2Mg_8Si_7$) and π-phase ($Al_8Mg_3FeSi_6$) remained unchanged both in acidic and basic medium. These observations of galvanic polarity reversal were consistent predictions obtained from potentiodynamic polarization tests as reported by Ikeuba and coworkers. However, there were significant discrepancies in the behavior of the intermetallic particles under near-neutral conditions; Apart from the Q-phase ($Al_4Cu_2Mg_8Si_7$) which remained cathodic in the galvanic couple, the β-phase (Al_3Mg_2) and η-phase ($MgZn_2$) and π-phase ($Al_8Mg_3FeSi_6$) displayed self-dissolution of the intermetallic particle in which both cathodic and anodic sides appeared on the intermetallic particle contrary to the assumption that intermetallic particle should be either anodic or cathodic as predicted by polarization curves. This indicates that the details of the localized electrochemical actives occurring on an IMP/Al couple surface are vital in giving a more accurate prediction of the consequence of the presence of the intermetallic particle in the aluminum alloy matrix. Hence the use of techniques such as the SVET and SIET are advocated to for a better interpretation of micro galvanic corrosion phenomena in aluminum alloys.

9 Persistent hydrogen evolution from Mg containing intermetallic compounds

In contrast to conventional activation-controlled electrochemical kinetics, the corrosion of magnesium and magnesium alloys under anodic polarization occurs with a sustained increase in the hydrogen evolution rate with increase in potential. The negative difference effect (NDE), also referred to as anodic hydrogen evolution (AHE), is the phenomena of faster hydrogen evolution on corroding magnesium surfaces. What causes this anodic hydrogen evolution is still unknown despite a great deal of research on this matter. Ikeuba *et al.*[183] used the hydrogen evolution technique and specially designed polarization schemes to study the anodic hydrogen evolution on Mg, $MgZn_2$ (η-phase), $Al_4Cu_2Mg_8Si_7$ (Q-phase), and Mg_2Si (β-phase) intermetallic compounds. The findings demonstrate that pure Mg and $MgZn_2$ exhibit higher hydrogen evolution rates at constant applied anodic current densities than do Q-phase and Mg_2Si, suggesting that AHE is not

© 2024 The Author(s). Published by the Royal Society of Chemistry

Open Access Article. Published on 09 October 2024. Downloaded on 7/19/2025 2:17:10 AM.
This article is licensed under a Creative Commons Attribution-NonCommercial 3.0 Unported Licence.

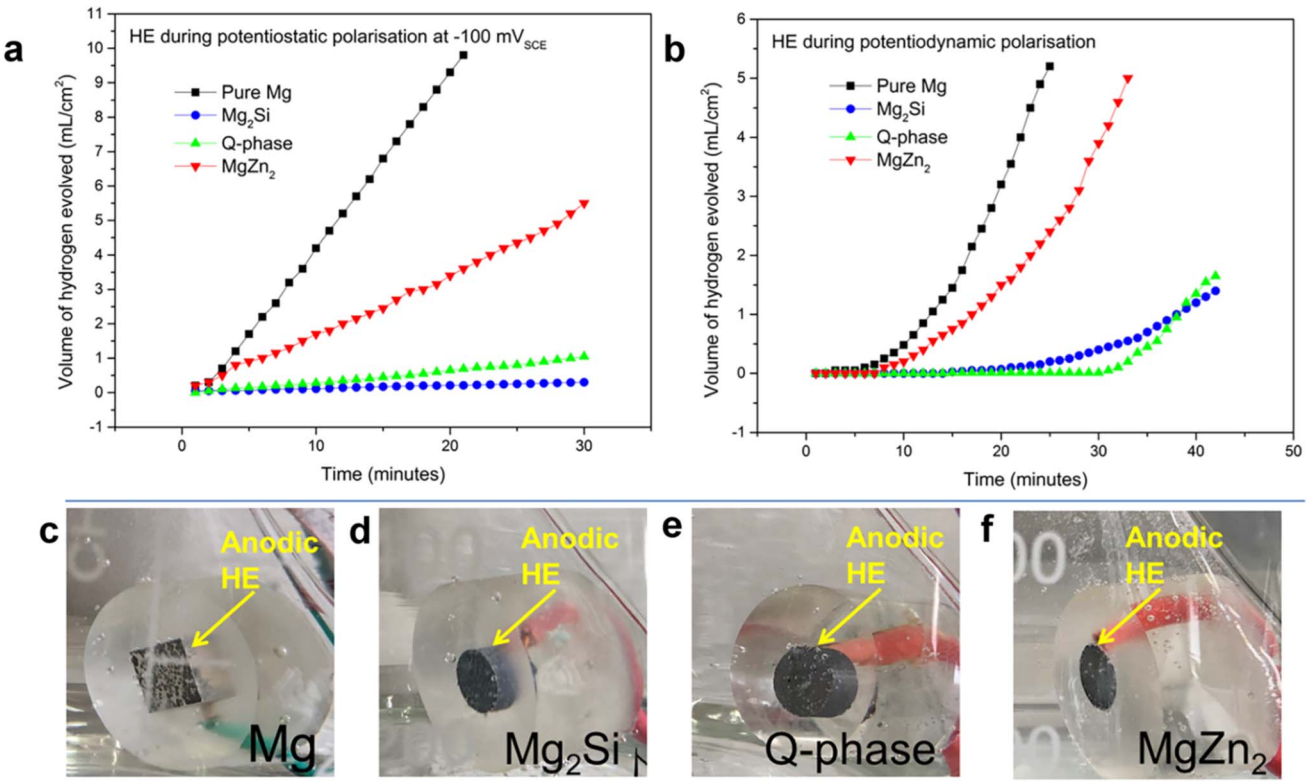

Fig. 18 Hydrogen evolution per surface area on pure Mg, Mg_2Si, Q-phase, and $MgZn_2$ electrodes during (a) potentiodynamic polarization, (b) potentiostatic polarization at – 100 mV_{SCE} (c), (d), (e), and (f) are photographs showing the evolution of hydrogen on the electrodes at – 100 mV_{SCE}. This figure has been adapted/reproduced from (ref. 183) with permission from Springer Nature, copyright 2024.

as prominent in these two phases (Fig. 18). Following anodic galvanostatic polarization, Mg, $MgZn_2$, and $Al_4Cu_2Mg_8Si_7$ showed clearly increased cathodic activity, while Mg_2Si showed no discernible change. The results of the stepped galvanostatic–potentiostatic tests show that pure magnesium exhibits the greatest degree of cathodic activity enhancement with an increase in applied anodic current density, followed by $MgZn_2$ and Q-phase. In contrast, Mg_2Si showed no discernible change in cathodic activity. It was determined that no single model could account for the simultaneous AHE of all the electrodes. However, in many circumstances, the observed experimental observations can be explained by any or a combination of two recently developed mechanisms; "enhanced catalytic activity mechanism" and the "incomplete film univalent Mg^+ ion mechanism".

10 Limitations in the electrochemical characterization of intermetallic compounds

Despite the wealth of electrochemical data and information provided by conventional techniques such as open circuit and polarization measurements, there still exists pertinent shortcomings which lie in its incapability to give the current density distribution over an active IMPs or alloy matrix, particularly in near-neutral conditions when numerous IMPs couples have been found to experience self-dissolution in the IMP/Al-alloy pair with no significant electrochemical activity on the alloy matrix. In addition, the polarization curves cannot forecast short-term variations in the galvanic polarity of a dissolving IMP/Al-alloy couple. Due to the failure in the capability of traditional electrochemical methods to provide the spatial resolution of the electrochemical reactivity on the galvanic couple surface, *in situ* approaches to obtain this information on a micro-scale are advocated. According to reports, the scanning vibrating electrode method (SVET) and the scanning ion-selective electrode technique (SIET) are appropriate for providing a spatial mechanistic insight into local currents and pH distribution, respectively. While SIET uses an ion-selective microelectrode to sense pH fluctuations on a surface, SVET uses a vibrating microelectrode to detect anodic and cathodic processes in active spots on surfaces. Recent literature reveals that scanning probe techniques have been successfully employed to evaluate the electrochemical and galvanic corrosion behavior of intermetallic compounds in the context of aluminum alloys. These scanning probe techniques could provide details of electrochemical activities on anodic and cathodic sites (current density distribution map) in addition to local ion distribution (H^+, Cl^-, Mg^{2+}, *etc.*). Meanwhile, the SVET/SIET is accompanied by technical issues such as when the cathode–anode spacing falls beneath the vibrating probe's resolution, the measured currents may be miscalculated and the evolution of the electrochemical activities misinterpreted. For instance, for the uncoupled intermetallic samples, defined

Open Access Article. Published on 09 October 2024. Downloaded on 7/19/2025 2:17:10 AM.
This article is licensed under a Creative Commons Attribution-NonCommercial 3.0 Unported Licence.

peaks for anodic and cathodic zones may not be noted due to some form of uniform corrosion leading to wrong estimates of current densities.

11 Research gap in the investigation of IMPs

Inaccurate prediction of galvanic polarity and activity-most of the reports in the literature indicates that investigations on IMPs were by open circuit and polarization measurements except for fewer more recent research. This leaves a wide gap of inaccurate predictions of galvanic polarity as these conventional methods fail to provide this information. Also, polarization measurements are not an exceptionally reliable parameter to predict the relative active or noble character of IMPs as demonstrated in the literature.

Disjointed reports on IMPs are disjointed and various research investigated different IMPs from different perspectives using various methods. Thus, there is a need a systematic study of IMPs occurring in a particular class of aluminum alloys to allow for more valid comparison and prediction.

Inadequate of information on the corrosion film formation-reports indicate that most research reports concentrated more on the corrosion potentiation and breakdown potential assessments. The film formation mechanism is an especially important and crucial part of understanding the corrosion mechanism of both the individual IMPs and in the context of Al-alloys.

12 Prospects and recommendations

Notwithstanding the current research effort towards understanding the corrosion characteristics of intermetallic compounds, certain aspects of the corrosion mechanism remain unclear due to inadequate information on the local electrochemical process occurring on the micro galvanic couples that are set up by intermetallic compounds. This information can be acquired using *in situ* scanning probe techniques which are capable of spatial resolution of the electrochemical processes occurring on the active surface as successfully used by some researchers. Scanning probe techniques can also offer researchers the opportunity to easily note galvanic polarity reversal under different conditions and detect the cases of self-dissolution of intermetallic compounds, especially under neutral conditions. Furthermore, the corrosion film development is a crucial aspect of understanding the dissolution mechanism of IMPs. This also calls for the implementation of surface-sensitive analytical techniques such as the XPS, ToF-SIMS and FIB-TEM which can provide information on thin fragile films. Hence, we recommend a combined approach to the investigation of IMPs using conventional for example in a recent study of the $MgZn_2$ phase, different film structures were observed at different potentials using potentiation polarization schemes, thanks to FIB-TEM which enabled the visualization and identification of the stratified films at different potentials.[7]

There is a need to investigate other intermetallic phases which coexist with the other intermetallic phases which have not been reported in the literature. This is to gain a holistic and more reliable interpretation of the electrochemical consequence of the presence of these phases in aluminum alloy. For example, when the S-phase and $Al_{20}Cu_2Mn_3$ coexist, if the size of the S-phase is between 2–10 nm, the $Al_{20}Cu_2Mn_3$ assumes the main role in local corrosion propagation, on the other hand, if the size of the S-phase is greater than 10 nm, both the S-phase and $Al_{20}Cu_2Mn_3$ actively contribute to the localized corrosion features of the alloy matrix.

Although there are few attempts in the literature to investigate the anodic hydrogen evolution (AHE) of magnesium-containing compounds,[183] the information on the AHE of many magnesium containing IMPs remains limited, thus there should be intensified efforts towards this area to gain the understanding needed for a more accurate interpretation of the electrochemical interfacial phenomena.[183] This is indeed important because the corrosion of aluminum is pH sensitive and AHE causes local alkalization which changes the near-surface pH which can change the electrochemical characteristics of the dissolving alloy surface.

13 Conclusion

Reviewed reports on the electrochemical and the galvanic/bimetallic corrosion behavior of important intermetallic compounds in the context of aluminum alloys revealed that there have been several research efforts geared towards this subject matter. Different researchers approached the subject from different perspectives and the investigations are to different extents. Some focused on the investigations using surface characterization, spectroscopic techniques, and conventional electrochemical techniques. More recent reports revealed the incorporation of scanning probe techniques which revealed more about the electrochemical activities on the active alloy surface thereby limiting the shortcomings of prior methods. Findings herein indicate that intermetallic phases play a predominant role in localized corrosion initiation and propagation in aluminum-based alloys in differing environments. This review has provided additional insights into the microstructural consequence of the presence of intermetallic compounds in aluminum alloys. The size, distribution, and composition of the intermetallic phases were noted to have a pronounced impact on the electrochemical characteristics of the bulk alloy. The pH of the environment plays a crucial role in the dissolution behavior of the intermetallic phases as there were remarkable differences with a change in pH. Indeed, to forecast and manage the corrosion susceptibility of Al alloys, it is important to have a deepened understanding of the unique properties of intermetallic particles and how they interact with the aluminum matrix in different environments.

Data availability

We declare that all associated data will be made available on reasonable request.

© 2024 The Author(s). Published by the Royal Society of Chemistry

Open Access Article. Published on 09 October 2024. Downloaded on 7/19/2025 2:17:10 AM. This article is licensed under a Creative Commons Attribution-NonCommercial 3.0 Unported Licence.

Author contributions

Alexander I. Ikeuba – conceptualization, project administration, writing of original draft, review and editing. Chigoziri N. Njoku – writing of original draft. Okpo O. Ekerenam – writing of original draft. Damian N. I. Njoku – writing of original draft. Inime I. Udoh – writing of original draft, review and editing. Enobong F. Daniel – writing of original draft. Paul C. Uzoma – writing of original draft, review and editing. Ini-ibehe N. Etim – writing of original draft, review and editing. Bright O. Okonkwo – writing of original draft, review and editing.

Conflicts of interest

There are conflicts of interest among the authors.

Acknowledgements

This research did not receive any form of funding.

References

1 R. G. Buchheit, A Compilation of Corrosion Potentials Reported for Intermetallic Phases in Aluminum Alloys, *J. Electrochem. Soc.*, 1995, **142**, 3994.
2 L. G. Bland, N. Birbilis and J. R. Scully, Exploring the Effects of Intermetallic Particle Size and Spacing on the Corrosion of Mg–Al Alloys Using Model Electrodes, *J. Electrochem. Soc.*, 2016, **163**, C895–C906.
3 R. G. Buchheit, *et al.*, Local dissolution phenomena associated with S phase (Al_2CuMg) particles in aluminum alloy 2024-T3, *J. Electrochem. Soc.*, 1997, **144**, 2621–2628.
4 L. F. Mondolfo, *The Aluminum–Magnesium–Zinc*, Revere Copper and Brass Inc., Rome, NY, 1967.
5 N. Birbilis and R. G. Buchheit, Investigation and Discussion of Characteristics for Intermetallic Phases Common to Aluminum Alloys as a Function of Solution pH, *J. Electrochem. Soc.*, 2008, **155**, C117.
6 J. A. Lyndon, R. K. Gupta, M. A. Gibson and N. Birbilis, Electrochemical behaviour of the β-phase intermetallic (Mg_2Al_3) as a function of pH as relevant to corrosion of aluminium–magnesium alloys, *Corros. Sci.*, 2013, **70**, 290–293.
7 A. I. Ikeuba, F. Kou, H. Duan, B. Zhang, J. Wang, E.-H. Han and W. Ke, Understanding the Electrochemical behavior of $MgZn_2$ as a function of pH, *J. Solid State Electrochem.*, 2019, **23**(4), 1165–1177.
8 A. I. Ikeuba, B. Zhang, J. Wang, E.-H. Han and W. Ke, Understanding the galvanic corrosion of the Q-phase/Al couple using SVET and SIET, *J. Mater. Sci. Technol.*, 2019, **35**(7), 1444–1454.
9 C. M. Liao and R. P. Wei, Galvanic coupling of model alloys to aluminum—a foundation for understanding particle-induced pitting in aluminum alloys, *Electrochim. Acta*, 1999, **45**, 881–888.
10 M. Liu, P. Schmutz, S. Zanna, A. Seyeux, H. Ardelean, G. Song, A. Atrens and P. Marcus, Electrochemical reactivity, surface composition and corrosion mechanisms of the complex metallic alloy Al_3Mg_2, *Corros. Sci.*, 2010, **52**, 562–578.
11 J. Li, N. Birbilis and R. G. Buchheit, Electrochemical assessment of interfacial characteristics of intermetallic phases present in aluminium alloy 2024-T3, *Corros. Sci.*, 2015, **101**, 155–164.
12 N. Birbilis and R. G. Buchheit, Electrochemical Characteristics of Intermetallic Phases in Aluminum Alloys, *J. Electrochem. Soc.*, 2005, **152**, B140.
13 A. I. Ikeuba, B. Zhang, J. Wang, E.-H. Han and W. Ke, Electrochemical, TOF-SIMS and XPS studies on the corrosion behavior of the Q-phase, *Appl. Surf. Sci.*, 2019, **490**, 535–545.
14 A. I. Ikeuba, B. Zhang and B. I. Ita, SVET and ToF-SIMS Studies on the Galvanic Corrosion of β-phase/Aluminum Couple in Aqueous Solutions as a Function of pH, *J. Electrochem. Soc.*, 2020, **167**(2), 021507.
15 A. I. Ikeuba, J. E. Ntibi, P. C. Okafor, B. I. Ita, A. U. Agobi, F. C. Asogwa, B. J. Omang, E. A. Eno, H. Loius, S. A. Adalikwu, B. A. Abiola, F. E. Abeng and N. A. Abang, Kinetic and Thermodynamic Evaluation of Azithromycin as a Green Corrosion Inhibitor during Acid Cleaning Process of Mild Steel using an Experimental and Theoretical Approach, *Results Chem.*, 2023, **5**, 100909.
16 A. I. Ikeuba, C. U. Sonde, I. E. Chukwudubem, R. C. Anozie, B. U. Ugi, I. B. Onyeachu, O. O. Ekerenam and W. Emori, Electrochemical evaluation of the anti-corrosion potential of selected amino acids on the magnesium in aqueous sodium chloride solutions, *Anti-Corros. Methods Mater.*, 2023, **70**(5), 252–258.
17 I. C. Ukaga, P. C. Okafor, I. B. Onyeachu, A. I. Ikeuba and D. I. Njoku, The inhibitive performance of 2,3-pyrazinedicarboxylic acid and synergistic impact of KI during acid corrosion of 70/30 and 90/10 copper–nickel alloys, *Mater. Chem. Phys.*, 2023, **296**, 127313.
18 V. M. Udowo, M. Yang, F. Liu and A. I. Ikeuba, Corrosion under insulation of pipeline steel in groundwater containing sulphate-reducing bacteria, *Corros. Eng., Sci. Technol.*, 2023, **56**(6), 549–560.
19 C. N. Njoku, B. N. Enendu, S. J. Okechukwu, N. Igboko, S. O. Anyikwa, A. I. Ikeuba, I. B. Onyeachu, I. I. N. Etim and D. I. Njoku, Review on anti-corrosion properties of expired antihypertensive drugs as benign corrosion inhibitors for metallic materials in various environments, *Results Eng.*, 2023, **18**, 101183.
20 A. A. Bamigbola, A. I. Ikeuba, M. E. Ikpi, C. E. Gimba and G. A. Shallangwa, Gravimetric and electrochemical study of clindamycin as corrosion inhibitor for mild steel in acidic media, *Arch. Metall. Mater.*, 2023, **69**, DOI: 10.24425/amm.2024.151414.
21 A. I. Ikeuba, B. J. Omang, V. M. Bassey, H. Louis, A. U. Agobi, J. E. Ntibi and F. C. Asogwa, Experimental and theoretical evaluation of Aspirin as a green corrosion inhibitor for mild steel in acidic medium, *Results Chem.*, 2022, **4**, 100543.

Open Access Article. Published on 09 October 2024. Downloaded on 7/19/2025 2:17:10 AM. This article is licensed under a Creative Commons Attribution-NonCommercial 3.0 Unported Licence.

22 A. I. Ikeuba, A. U. Agobi, H. Louis, F. C. Asogwa, B. J. Omang and M. Udoiyang, Green approach towards corrosion inhibition of mild steel during acid pickling using chlorpheniramine: experimental and DFT study, *Chem. Afr.*, 2022, **6**, 983–997.

23 I. N. Etim, D. I. Njoku, P. C. Uzoma, S. K. Kolawole, O. S. Olanrele, O. O. Ekarenem, B. O. Okonkwo, A. I. Ikeuba, I. I. Udoh, C. N. Njoku and W. Emori, Microbiologically Influenced Corrosion: A concern for oil and gas sector in Africa, *Chem. Afr.*, 2022, **6**, 779–804.

24 I. K. Nwokolo, H. Shi, A. I. Ikeuba, N. Gao, J. Li, S. Ahmed and F. Liu, Synthesis, characterization, and investigation of anti-corrosion properties of an innovative metal-organic framework ZnMOF-BTA on carbon steel in HCl solution, *Coatings*, 2022, **12**(9), 1288.

25 V. M. Udowo, M. Yang, F. Liu and A. I. Ikeuba, Corrosion under insulation of pipeline steel in groundwater containing sulphate-reducing bacteria, *Corros. Eng., Sci. Technol.*, 2023, **58**(6), 549–560.

26 V. M. Udowo, M. Yang, F. Liu and A. I. Ikeuba, Role of Fe oxide in the underdeposit corrosion of pipeline steel in oilfield produced water containing SRB, *Mater. Corros.*, 2022, **75**(1), 118–129.

27 F. E. Abeng, M. E. Ikpi, P. C. Okafor, V. C. Anadebe, K. J. Uwakwe, A. I. Ikeuba and N. A. Okafor, Corrosion inhibition of API 5L X-52 steel in oilfield acidizing solution by Gentamicine and sulfamethoxazole: experimental, plane-wave density functional theory (PWDFT) and the generalized-gradient approximation (GGA) simulations, *J. Adhes. Sci. Technol.*, 2021, **36**(22), 2438–2461.

28 U. B. Essien, M. E. Ikpi, A. I. Ikeuba and N. B. Essien, Experimental and Computational Chemistry investigations of tartaric acid as green corrosion inhibitor for API 5L X 52 carbon steel in 0.5 M HCl, *Commun. – R. Soc. Edinburgh, Phys. Sci.*, 2021, **7**(4), 482–193.

29 P. Adapala, T. Avey, Y. Yuan, M. L. Lim, G. Bhaskaran, S. Das, A. Luo and G. S. Frankel, Understanding the effect of microstructure and composition on localized corrosion susceptibility of 6xxx aluminum alloys, *npj Mater. Degrad.*, 2024, **8**(1), 52.

30 I. I. Udoh, H. Shi, M. Soleymanibrojeni, F. Liu and E.-H. Han, Inhibition of galvanic corrosion in Al/Cu coupling model by synergistic combination of 3-amino-1,2,4-triazole-5-thiol and cerium chloride, *J. Mater. Sci. Technol.*, 2020, **44**, 102–115.

31 A. Kosari, F. Tichelaar, P. Visser, H. Zandbergen, H. Terryn and J. M. C. Mol, Dealloying-driven local corrosion by intermetallic constituent particles and dispersoids in aerospace aluminium alloys, *Corros. Sci.*, 2020, **177**, 108947.

32 Y. Li, T. Zhang and F. Wang, Unveiling the effect of Al–Mn intermetallic on the micro-galvanic corrosion of AM50 Mg alloy in NaCl solution, *J. Mater. Res. Technol.*, 2023, **26**, 753–763.

33 R. Ly, K. T. Hartwig and H. Castaneda, Effects of strain localization on the corrosion behavior of ultra-fine grained aluminum alloy AA6061, *Corros. Sci.*, 2018, **139**, 47–57.

34 K. Zhao, G. Han, T. Gao, H. Yang, Z. Qian, K. Hu, G. Liu, J. Nie and X. Liu, Interface precipitation and corrosion mechanisms in a model Al–Zn–Mg–Cu alloy strengthened by TiC particles, *Corros. Sci.*, 2022, **206**, 110533.

35 K. A. Yasakau, M. L. Zheludkevich and M. G. S. Ferreira, Role of intermetallics in corrosion of aluminum alloys. Smart corrosion protection, in *Intermetallic Matrix Composites*, Elsevier, 2018, DOI: **10.1016/B978-0-85709-346-2.00015-7**.

36 S. H. Kayani, H.-Y. Ha, B.-J. Kim, Y.-H. Cho, H.-W. Son and J.-M. Lee, Impact of intermetallic phases on the localised pitting corrosion and high-temperature tensile strength of Al–SiMgCuNi alloys, *Corros. Sci.*, 2024, **233**, 112064.

37 X. Xiao, Z. Zhou, C. Liu and L. Cao, Microstructure and Its Effect on the Intergranular Corrosion Properties of 2024-T3 Aluminum Alloy, *Crystals*, 2022, **12**(3), 395.

38 C. Brito, T. Vida, E. Freitas, N. Cheung, J. E. Spinelli and A. Garcia, Cellular/dendritic arrays and intermetallic phases affecting corrosion and mechanical resistances of an Al–Mg–Si alloy, *J. Alloys Compd.*, 2016, **673**, 220–230.

39 J. Li, N. Birbilis and R. G. Buchheit, Electrochemical assessment of interfacial characteristics of intermetallic phases present in aluminium alloy 2024-T3, *Corros. Sci.*, 2015, **101**, 155–164.

40 J. Wang, B. Zhang, B. Wu and X. L. Ma, Size-dependent role of S phase in pitting initiation of 2024Al alloy, *Corros. Sci.*, 2016, **105**, 183–189.

41 Y. Liew, C. Örnek, J. Pan, D. Thierry, S. Wijesinghe and D. J. Blackwood, Towards understanding micro-galvanic activities in localised corrosion of AA2099 aluminium alloy, *Electrochim. Acta*, 2021, **392**, 139005.

42 A. Chemin, D. Marques, L. Bisanha, A. de J. Motheo, W. W. Bose Filho and C. O. F. Ruchert, Influence of Al_7Cu_2Fe intermetallic particles on the localized corrosion of high strength aluminum alloys, *Mater. Des.*, 2014, **53**, 118–123.

43 J. Sieniawski, Microstructure and mechanical properties of C355:0 cast aluminium alloy, *Arch. Mater. Sci. Eng.*, 2011, **47**, 85–94.

44 D. G. Harlow, R. P. Wei and M. Z. Wang, Statistical analysis of constituent particles in 7075-T6 aluminum alloy, *Metall. Mater. Trans. A*, 2006, **37**, 3367–3373.

45 K. Jones and D. W. Hoeppner, The interaction between pitting corrosion, grain boundaries, and constituent particles during corrosion fatigue of 7075-T6 aluminum alloy, *Int. J. Fatigue.*, 2009, **31**, 686–692.

46 Y. Tan, N. N. Aung and T. Liu, Novel corrosion experiments using the wire beam electrode. (I) Studying electrochemical noise signatures from localised corrosion processes, *Corros. Sci.*, 2006, **48**, 23–38.

47 M. Wang, M. Y. Tan, Y. Zhu and Y. Huang, Probing top-of-the-line corrosion using coupled multi-electrode array in conjunction with local electrochemical measurement,*npj*, *Mater. Degrad.*, 2023, 1–16.

© 2024 The Author(s). Published by the Royal Society of Chemistry

Open Access Article. Published on 09 October 2024. Downloaded on 7/19/2025 2:17:10 AM. This article is licensed under a Creative Commons Attribution-NonCommercial 3.0 Unported Licence.

48 A. I. Ikeuba and P. C. Okafor, Green corrosion protection for mild steel in acidic media: saponins and crude extracts of Gongronemalatifolium, *Pigm. Resin Technol.*, 2018, **48**(1), 57–64.

49 B. U. Ugi, M. E. Obeten and A. I. Ikeuba, Inhibition Efficiency of Eco-friendly Green Inhibitors (Ocimumtenuiflorum Phytocompounds) on Corrosion of High Carbon Steel in HCl Environment using Thermometric and Electrochemical Methods, *Adv. Electrochem.*, 2018, **4**(1), 158–161.

50 K. J. Uwakwe, P. C. Okafor, A. I. Obike and A. I. Ikeuba, Molecular Dynamic Simulation and Quantum Chemical Calculations for the Adsorption of some Imidazoline Derivatives on Iron Surface, *Global J. Pure Appl. Sci.*, 2017, **23**, 69–80.

51 A. I. Ikeuba, B. I. Ita, P. C. Okafor, V. M. Bassey, B. U. Ugi and E. B. Kporokpo, Green Corrosion Inhibitors for Mild Steel in H2SO4 Solution: Flavonoids of Gongronemalatifolium, *Prot. Met. Phys. Chem. Surf.*, 2015, **51**(6), 1043–1049.

52 B. U. Ugi, E. Jackson, A. I. Ikeuba and I. E. Uwah, Mangifera indica Leave Extracts as Organic Inhibitors on the Corrosion of Zinc Sheet in 5 M H2SO4 Solution, *J. Appl. Sci. Environ. Manage.*, 2015, **19**(1), 145–152.

53 P. C. Okafor, U. C. Udoh, A. I. Ikeuba and U. J. Ekpe, The Inhibition of Mild Steel Corrosion by Extracts from Seeds of Myristica fragrance, Monodora mystica and Parkia biglobosa in Sulphuric Acid Solution, *ASUU J. Sci.*, 2014, **2**(1), 34–46.

54 P. C. Okafor, A. I. Ikeuba, N. E. Nya and U. J. Ekpe, Ethanol Extracts from Piper guineense as Green Corrosion Inhibitor of Mild Steel in Sulphuric Acid Solution, *ASUU J. Sci.*, 2014, **2**(1), 79–98.

55 A. I. Ikeuba, P. C. Okafor, U. J. Ekpe and E. E. Ebenso, Alkaloid and non-alkaloid ethanolic extracts from seeds of Garcinia kola as green corrosion inhibitors of mild steel in H2SO4 solution, *Int. J. Electrochem. Sci.*, 2013, **8**, 7455–7467.

56 I. E. Uwah, B. U. Ugi, P. C. Okafor and A. I. Ikeuba, Investigation of the corrosion inhibition effects of bitters on mild steel in acidic media: a case study of Andrographis paniculata and Vernonia amygdalina, *Int. J. Appl. Chem.*, 2013, **9**(1), 73–88.

57 P. C. Okafor, P. U. Okon, E. F. Daniel, A. I. Ikeuba and U. J. Ekpe, Adsorption capacity of periwinkle (Tympanotonusfuscatus) shell for lead, copper, cadmium and arsenic from aqueous solutions, *J. Chem. Soc. Niger.*, 2013, **38**(1), 77–84.

58 I. E. Uwah, A. I. Ikeuba, B. U. Ugi and V. M. Udowo, Comparative study of the inhibition effects of alkaloid and non alkaloid fractions of the ethanolic extracts of Costusafer stem on the corrosion of mild steel in 5 M HCl solution, *Global J. Pure Appl. Sci.*, 2013, **19**, 23–32.

59 I. E. Uwah, B. U. Ugi, A. I. Ikeuba and U. B. Essien, Costusafer leave extract as Nontoxic Corrosion Inhibitor for mild steel in H2SO4 Solution, *Global J. Pure Appl. Sci.*, 2013, **19**, 119–127.

60 F. E. Abeng, U. J. Ekpe, A. I. Ikeuba, B. U. Ugi and P. J. Nna, Inhibitive Action of Alkaloids and Non Alkaloid Fractions of the Ethanolic Extracts of Phyllanthus amarus on the Corrosion of Mild Steel in HCl Solution, *Global J. Pure Appl. Sci.*, 2013, **19**, 107–117.

61 I. K. Nwokolo, H. Shi, A. I. Ikeuba, W. Zhang, F. Liu and E.-H. Han, A polyurethane coating using CoMOF-BTA metal-organic framework for active protection of AA2024-T3, *J. Coat. Technol. Res.*, 2023, **21**, 521–535.

62 W. Emori, I. I. Udoh, O. O. Ekerenam, A. I. Ikeuba, I. N. Etim, C. N. Njoku, E. F. Daniel, D. I. Njoku, P. C. Uzoma, S. K. Kolawole and O. S. Olanrele, Handling heat-stable salts in post-combustion CO_2 capture: a detailed survey, *Greenhouse Gases: Sci. Technol.*, 2023, **13**(6), 876–904.

63 P. C. Uzoma, I. N. Etim, B. O. Okonkwo, O. S. Olanrele, D. I. Njoku, S. K. Kolawole, W. Emori, A. I. Ikeuba, C. N. Njoku, O. O. Ekerenam, I. P. Etim, E. F. Daniel and I. I. Udoh, Recent design approaches, adhesion mechanisms, and applications of antibacterial surfaces, *Chem. Eng. J. Adv.*, 2023, **16**, 100563.

64 N. E. Nya, A. I. Ikeuba, P. C. Okafor, B. U. Ugi, V. M. Bassey and A. I. Obike, Mild Steel Corrosion Mitigation in Sulphuric Acid *via* Benign Isolated Phytochemicals from Viscum album, *J. Mater. Sci. Chem. Eng.*, 2018, **6**, 132–146.

65 L. Aondoakaa and A. I. Ikeuba, Evaluation of adsorption behavior of selected amino acids on magnesium using DFT and molecular dynamics simulations, *2nd Conference on Physical Sciences*, UNICAL FPS-2023, Calabar, 2023.

66 D. A. Lytle and W. H. Lee, Sarah Singer, States, the Law and Access to Refugee Protection: Fortresses and Fairness. Edited by Maria O'Sullivan and Dallal Stevens, *Migr. Stud.*, 2019, **10**(2), 298–301.

67 C. Mondal and A. K. Mukhopadhyay, Annealed 7055 aluminum alloy On the ature of T(Al2Mg3Zn3) and S(Al2CuMg) phases present in as-cast and annealed 7055 aluminum alloy, *Mater. Sci. Eng. A*, 2005, **39**(1), 367–376.

68 D. H. Chun, Y. Xu, M. Demura and K. Kishida, Catalytic Properties of Ni 3 Al Foils for Methanol Decomposition Catalytic properties of Ni_3 Al foils for methanol decomposition, *Catal. Lett.*, 2006, **106**, 71–75.

69 E. Cambril, A. Chovin and C. Demaille, Touching Surface-Attached Molecules with a Microelectrode : Mapping the Distribution of Redox-Labeled Macromolecules by Electrochemical-Atomic Force Microscopy, *Anal. Chem.*, 2010, **82**(15), 6353–6362.

70 F. Wang, F. Wang, D. G. Eskin, A. V. Khvan, K. F. Starodub, J. J. H. Lim, M. G. Burke, T. Connolley and J. Mi, On the occurrence of a eutectic-type structure in solidification of Al–Zr alloys Scripta Materialia On the occurrence of a eutectic-type structure in solidi fi cation of Al–Zr alloys,Scripta, *Materialia*, 2017, **133**, 75–78.

71 M. Abubakar and M. A. Onimisi, Effect of Precipitation Hardening Treatment on Corrosion Behavior and Anodic Efficiency of Sacrificial Anode Produced from Recycled Al–Zn–Mg Alloy, *J. Fail. Anal. Prev.*, 2021, **21**, 1212–1219.

Open Access Article. Published on 09 October 2024. Downloaded on 7/19/2025 2:17:10 AM. This article is licensed under a Creative Commons Attribution-NonCommercial 3.0 Unported Licence.

72 A. I. Ikeuba, F. Kou, H. Duan, B. Zhang, J. Wang, E. Han and W. Ke, Understanding the electrochemical behavior of bulk-synthesized MgZn2 intermetallic compound in aqueous NaCl solutions as a function of pH, *J. Solid State Electrochem.*, 2019, **23**, 1165–1177.

73 A. I. Ikeuba, B. Zhang, P. C. Okafor, J. Wang, E. Han and W. Ke, SVET and SIET Study of Galvanic Corrosion of Al/MgZn 2 in Aqueous Solutions at Different pH SVET and SIET Study of Galvanic Corrosion of Al/MgZn 2 in Aqueous Solutions at Different pH, *J. Electrochem. Soc.*, 2018, **165**(3), 165–180.

74 A. I. Ikeuba, B. Zhang, J. Wang, E. Han and W. Ke, Journal of Materials Science & Technology Understanding the galvanic corrosion of the Q-phase/Al couple using SVET and SIET, *J. Mater. Sci. Technol.*, 2019, **35**, 1444–1454.

75 A. I. Ikeuba, Applied Surface Science Advances AFM and EIS investigation of the influence of pH on the corrosion film stability of Al 4 Cu 2 Mg 8 Si 7 intermetallic particle in aqueous solutions, *Appl. Surf. Sci. Adv.*, 2022, **11**, 100291.

76 J. Huang, S. Feng, S. Li, C. Wu and J. Chen, The crystallographic corrosion and its microstructure in an Al–Cu–Li alloy, *J. Alloys Compd.*, 2021, **861**, 158588.

77 F. Wen, J. Chen, S. Zhong, Z. Zhou, S. Han, H. Wei, Y. Zhang, W. Li and R. Guan, Effect of crystal orientations and precipitates on the corrosion behavior of the Al–Cu alloy using single crystals, *J. Alloys Compd.*, 2021, **890**, 161858.

78 J. Sieniawski, Analysis of intermetallic particles in AlSi1MgMn aluminium alloy, *J. Achiev. Mater. Manuf. Eng.*, 2007, **20**, 155–158.

79 G. Mrówka-Nowotnik, Intermetallic phase particles in cast AlSi5Cu1Mg and AlCu4Ni2Mg2 aluminium alloys, *Arch. Mater. Sci. Eng.*, 2009, **38**, 69–77.

80 Y.-L. Cheng, C.-Y. Lee, Y.-L. Huang, C. A. Buckner, R. M. Lafrenie, J. A. Dénommée, J. M. Caswell, D. A. Want, G. G. Gan, Y. C. Leong, P. C. Bee, E. Chin, A. K. H. Teh, S. Picco, L. Villegas, F. Tonelli, M. Merlo, J. Rigau, D. Diaz, M. Masuelli, S. Korrapati, P. Kurra, S. Puttugunta, S. Picco, L. Villegas, F. Tonelli, M. Merlo, J. Rigau, D. Diaz, M. Masuelli, M. Tascilar, F. A. de Jong, J. Verweij and R. H. J. Mathijssen, *We Are IntechOpen, the World S Leading Publisher of Open Access Books Built by Scientists, for Scientists TOP 1%*, Intech, 2016, vol. 11, p. 13, **https://www.intechopen.com/books/advanced-biometric-technologies/liveness-detection-in-biometrics**.

81 J. Sieniawski and M. Wierzbińska, Morphology prediction of intermetallics formed in 4xxx type of aluminium alloy, *Manuf. Eng.*, 2008, **31**, 262–268.

82 Y. G. Son, S. S. Jung, Y. H. Park and Y. C. Lee, Effect of Semi-Solid Processing on the Microstructure and Mechanical Properties of Aluminum Alloy Chips with Eutectic Mg_2Si Intermetallics, *Metals*, 2021, **11**, 1414.

83 S. Kim, G. Lee, G. Park, H. Kim, A. Lee, K. G. Prashanth, D. Kim, J. Eckert and M. Lee, High strength nanostructured Al-based alloys through optimized processing of rapidly quenched amorphous precursors, *Sci. Rep.*, 2018, 1–12.

84 P. Cornette, S. Zanna, A. Seyeux, D. Costa and P. Marcus, The native oxide fi lm on a model aluminium–copper alloy studied by XPS and ToF-SIMS, *Corros. Sci.*, 2020, **174**, 108837.

85 F. Andreatta, H. Terryn and J. H. W. de Wit, Effect of solution heat treatment on galvanic coupling between intermetallics and matrix in AA7075-T6, *Corros. Sci.*, 2003, **45**, 1733–1746.

86 Q. Meng and G. S. Frankel, Effect of Cu Content on Corrosion Behavior of 7xxx Series Aluminum Alloys, *J. Electrochem. Soc.*, 2004, **151**, B271.

87 R. Ambat, A. J. Davenport, G. M. Scamans and A. Afseth, Effect of iron-containing intermetallic particles on the corrosion behaviour of aluminium, *Corros. Sci.*, 2006, **48**, 3455–3471.

88 J. A. Lyndon, R. K. Gupta, M. A. Gibson and N. Birbilis, Electrochemical behaviour of the β-phase intermetallic (Mg2Al3) as a function of pH as relevant to corrosion of aluminium-magnesium alloys, *Corros. Sci.*, 2013, **70**, 290–293.

89 K. Zhou, B. Wang, Y. Zhao and J. Liu, Corrosion and electrochemical behaviors of 7A09 Al–Zn–Mg–Cu alloy in chloride aqueous solution, *Trans. Nonferrous Met. Soc.*, 2015, 2509–2515.

90 N. Birbilis, M. K. Cavanaugh and R. G. Buchheit, Electrochemical behavior and localized corrosion associated with Al7Cu2Fe particles in aluminum alloy 7075-T651, *Corros. Sci.*, 2006, **48**, 4202–4215.

91 C. F. Mallinson, P. M. Yates, M. A. Baker, J. E. Castle, A. Harvey and J. F. Watts, The localised corrosion associated with individual second phase particles in AA7075-T6: a study by SEM, EDX, AES, SKPFM and FIB-SEM, *Mater. Corros.*, 2017, **68**, 748–763.

92 N. Birbilis and R. G. Buchheit, Electrochemical Characteristics of Intermetallic Phases in Aluminum Alloys, *J. Electrochem. Soc.*, 2005, **152**, B140.

93 N. Birbilis and R. G. Buchheit, Investigation and Discussion of Characteristics for Intermetallic Phases Common to Aluminum Alloys as a Function of Solution pH, *J. Electrochem. Soc.*, 2008, **155**, C117.

94 Z. Jin, C. Cai, T. Hashimoto, Y. Yuan, D. H. Kang, J. Hunter and X. Zhou, The behaviour of iron-containing intermetallic particles in aluminium alloys in alkaline solution, *Corros. Sci.*, 2021, **179**, 109134.

95 G. Šekularac, J. Kovač and I. Milošev, Comparison of the Electrochemical Behaviour and Self-sealing of Zirconium Conversion Coatings Applied on Aluminium Alloys of series 1xxx to 7xxx, *J. Electrochem. Soc.*, 2020, **167**, 111506.

96 K. D. Ralston, T. L. Young and R. G. Buchheit, Electrochemical Evaluation of Constituent Intermetallics in Aluminum Alloy 2024-T3 Exposed to Aqueous Vanadate Inhibitors, *J. Electrochem. Soc.*, 2009, **156**, C135.

97 Y. Zhu, K. Sun and G. S. Frankel, Intermetallic Phases in Aluminum Alloys and Their Roles in Localized Corrosion, *J. Electrochem. Soc.*, 2018, **165**, C807–C820.

98 I. N. Etim, D. I. Njoku, P. C. Uzoma, S. K. Kolawole, O. S. Olanrele, O. O. Ekarenem, B. O. Okonkwo,

© 2024 The Author(s). Published by the Royal Society of Chemistry

Open Access Article. Published on 09 October 2024. Downloaded on 7/19/2025 2:17:10 AM.
This article is licensed under a Creative Commons Attribution-NonCommercial 3.0 Unported Licence.

A. I. Ikeuba, I. I. Udoh, C. N. Njoku, I. P. Etim and W. Emori, Microbiologically Influenced Corrosion: A Concern for Oil and Gas Sector in Africa, *Chem. Afr.*, 2022.

99 I. N. Etim, J. Wei, J. Dong, D. Xu, N. Chen, X. Wei, M. Su and W. Ke, Mitigation of the corrosion-causing Desulfovibrio desulfuricans biofilm using an organic silicon quaternary ammonium salt in alkaline media simulated concrete pore solutions, *Biofouling*, 2019, 1–17.

100 C. Duan, J. Tang, W. Ma, L. Ye, H. Jiang, Y. Deng and X. Zhang, Intergranular corrosion behavior of extruded 6005A alloy profile with different microstructures, *J. Mater. Sci.*, 2020, **55**, 10833–10848.

101 K. M. Fleming, A. Zhu and J. R. Scully, Corrosion of AA6061 Brazed with an Al–Si Alloy: Effects of Si on Metallurgical and Corrosion Behavior, *Corrosion*, 2012, **68**, 1126–1145.

102 A. I. Ikeuba, P. C. Okafor, B. Ita, A. I. Obike, F. E. Abeng, U. Essien and A. Bamigbola, In situ SVET studies on the current density distribution on dissolving of Mg, MgZn, MgSi and AlCuMgSi surfaces in NaCl solutions, *Anti-Corros. Methods Mater.*, 2022, **69**, 104–110.

103 A. I. Ikeuba, Bimetallic corrosion evaluation of the π-$Al_8Mg_3FeSi_6$ phase/Al couple in acidic, neutral and alkaline aqueous solutions using the scanning vibrating electrode technique, *Electrochim. Acta*, 2023, **449**, 142240.

104 T. O. Mbuya, B. O. Odera and S. P. Ng'ang'a, Influence of iron on castability and properties of aluminium silicon alloys: literature review, *Int. J. Cast Met. Res.*, 2016, **16**, 451–465.

105 L. C. Lafortune, A feasibility study on the effect of an Al–C master alloy on the microstructure and mechanical properties of the B319 cast aluminum alloy, *Mater. Sci. Eng.*, 2019, DOI: **10.14288/1.0378583**.

106 V. A. Alza, Aging of Cast Aluminum Alloy A356: Effects on Mechanical Properties and Microstructure, *J. Mech. Eng. Sci.*, 2021, **18**, 54–65.

107 H. MÖLler, W. E. Stumpf and P. C. Pistorius, Influence of elevated Fe, Ni and Cr levels on tensile properties of SSM-HPDC Al–Si–Mg alloy F357, *Trans. Nonferrous Met. Soc. China*, 2010, **20**, s842–s846.

108 H. Zhou, *et al.*, Corrosion Behavior of the Al2Cu Intermetallic Compound and Coupled Al2Cu/Al, *Int. J. Electrochem. Sci.*, 2017, **12**(12), 9542–9554.

109 B. O. Okonkwo, H. Ming, F. Meng, J. Wang, X. Xu and E.-H. Han, Galvanic corrosion study between low alloy steel A508 and 309/308 L stainless steel dissimilar metals: a case study of the effects of oxide film and exposure time, *J. Nucl. Mater.*, 2021, **548**, 152853.

110 B. O. Okonkwo, H. Ming, J. Wang, F. Meng, X. Xu and E.-H. Han, Microstructural characterization of low alloy steel A508 – 309/308L stainless steel dissimilar weld metals, *Int. J. Press. Vessel. Pip.*, 2021, **190**, 104297.

111 J. Idrac, *et al.*, Galvanic corrosion of aluminium–copper model alloys, *Electrochim. Acta*, 2007, **52**, 7626–7633.

112 T. E. Graedel, *J. Electrochem. Soc*, 1989, **136**, 204c.

113 H. Shi, *et al.*, Simulating corrosion of Al2CuMg phase by measuring ionic currents, chloride concentration and pH, *Corros. Sci.*, 2014, **88**, 178–186.

114 R. G. Buchheit, *et al.*, Local dissolution phenomena associated with S phase (Al2CuMg) particles in aluminum alloy 2024-T3, *J. Electrochem. Soc.*, 1997, **144**, 2621–2628.

115 P. Schmutz and G. S. Frankel, Corrosion study of AA2024-T3 by scanning kelvin probe force microscopy and *in situ* atomic force microscopy scratching, *J. Electrochem. Soc.*, 1998, **145**, 2295–2306.

116 P. Leblanc and G. S. Frankel, A study of corrosion and pitting initiation of AA2024-T3 using atomic force microscopy, *J. Electrochem. Soc.*, 2002, **149**, B239–B247.

117 V. Guillaumin and G. Mankowski, Localized corrosion of 2024 T351 aluminium alloy in chloride media, *Corros. Sci*, 1999, **41**, 421–438.

118 D. Zhu and W. J. van Ooij, Corrosion protection of AA 2024-T3 by bis-[3-(triethoxysilyl)propyl]tetrasulfide in neutral sodium chloride solution. Part 1: corrosion of AA 2024-T3, *Corros. Sci*, 2003, **45**, 2163–2175.

119 M. H. Shao, *et al.*, A study on pitting corrosion of aluminum alloy 2024-T3 by scanning microreference electrode technique, *Mater. Sci. Eng. A*, 2003, **344**, 323–327.

120 A. Boag, *et al.*, Stable pit formation on AA2024-T3 in a NaCl environment, *Corros. Sci.*, 2010, **52**, 90–103.

121 N. Birbilis, *et al.*, Inhibition of AA2024-T3 on a phase-by-phase basis using an environmentally benign inhibitor, Cerium Dibutyl Phosphate, *Electrochem. Solid-State Lett.*, 2005, **8**, C180–C183.

122 F. H. Scholes, A. E. Hughes and D. Jamieson, Interaction of Ce(dbp)3 with surface of aluminium alloy 2024-T3 using macroscopic models of intermetallic phases, *Corros. Eng., Sci. Technol*, 2009, **44**, 416–424.

123 Y. Yoon and R. G. Buchheit, Dissolution behavior of Al2CuMg (S Phase) in chloride and chromate conversion coating solutions, *J. Electrochem. Soc.*, 2006, **153**, B151–B155.

124 J. G. Brunner, *et al.*, Impact of ultrafine-grained microstructure on the corrosion of aluminium alloy AA2024, *Corros. Sci.*, 2012, **57**, 209–214.

125 J. A. DeRose, *et al.*, Localised corrosion initiation and microstructural characterisation of an Al 2024 alloy with a higher Cu to Mg ratio, *Corros. Sci.*, 2012, **55**, 313–325.

126 X. Zhou, *et al.*, Study of localized corrosion in AA2024 aluminium alloy using electron tomography, *Corros. Sci.*, 2012, **58**, 299–306.

127 A. Boag, *et al.*, Corrosion of AA2024-T3 Part I: localised corrosion of isolated IM particles, *Corros. Sci.*, 2011, **53**, 17–26.

128 J. F. Li, *et al.*, Localized corrosion mechanism of 2000-series Al alloy containing S(Al2CuMg) and h0(Al2Cu) precipitates in 4.0% NaCl solution at pH 6.1, *Mater. Chem. Phys.*, 2005, **91**, 325–329.

129 P. Campestrini, *et al.*, Formation of a cerium based conversion coating on AA2024: relationship, with the microstructure, *Surf. Coat. Technol.*, 2004, **176**, 365–381.

130 J. H. W. de Wit, New knowledge on localized corrosion obtained from local measuring techniques, *Electrochim. Acta*, 2001, **46**, 3641–3650.

Open Access Article. Published on 09 October 2024. Downloaded on 7/19/2025 2:17:10 AM. This article is licensed under a Creative Commons Attribution-NonCommercial 3.0 Unported Licence.

131 P. Campestrini, *et al.*, Relation between microstructural aspects of AA2024 and its corrosion behaviour investigated using AFM scanning potential technique, *Corros. Sci.*, 2000, **42**, 1853–1861.
132 M. L. Zheludkevich, *et al.*, Triazole and thiazole derivatives as corrosion inhibitors for AA2024 aluminium alloy, *Corros. Sci.*, 2005, **47**, 3368–3383.
133 K. A. Yasakau, *et al.*, Mechanism of corrosion inhibition of AA2024 by rare-earth compounds, *J. Phys. Chem. B*, 2006, **110**, 5515–5528.
134 R. Goswami, *et al.*, Precipitation behavior of the ß phase in Al-5083, *Mater. Sci. Eng., A*, 2010, **527**(4), 1089–1095.
135 J. L. Searles, P. I. Gouma and R. G. Buchheit, Stress corrosion cracking of sensitized AA5083 (Al-4.5Mg-1.0Mn), *Metall. Mater. Trans. A*, 2001, **32**(11), 2859–2867.
136 I. N. A. Oguocha, O. J. Adigun and S. Yannacopoulos, Effect of sensitization heat treatment on properties of Al–Mg alloy AA5083-H116, *J. Mater. Sci.*, 2008, **43**(12), 4208–4214.
137 M. Seifi, *et al.*, Sensitization and remediation effects on environmentally assisted cracking of Al–Mg naval alloys, *Corros. Sci.*, 2018, **138**, 219–241.
138 J. A. Lyndon, *et al.*, Electrochemical behaviour of the β-phase intermetallic (Mg2Al3) as a function of pH as relevant to corrosion of aluminium–magnesium alloys, *Corros. Sci.*, 2013, **70**, 290–293.
139 Y. Li, *et al.*, pH-dependent electrochemical behaviour of Al3Mg2 in NaCl solution, *Appl. Surf. Sci.*, 2019, **467–468**, 619–633.
140 N. Birbilis and R. G. Buchheit, Electrochemical Characteristics of Intermetallic Phases in Aluminum Alloys: An Experimental Survey and Discussion, *J. Electrochem. Soc.*, 2005, **152**(4), B140.
141 R. G. Buchheit, A Compilation of Corrosion Potentials Reported for Intermetallic Phases in Aluminum Alloys, *J. Electrochem. Soc.*, 1995, **142**(11), 3994.
142 A. I. Ikeuba, B. Zhang and B. I. Ita, SVET and ToF-SIMS Studies on the Galvanic Corrosion of β-phase/Aluminum Couple in Aqueous Solutions as a Function of pH, *J. Electrochem. Soc.*, 2020, **167**(2), 021507.
143 T. He, *et al.*, Influence of Aging on Corrosion Behaviour of the 6061 Cast Aluminium Alloy, *Materials*, 2021, **14**(8), 1821.
144 F. Andreatta, H. Terryn and J. H. W. de Wit, Effect of solution heat treatment on galvanic coupling between intermetallics and matrix in AA7075-T6, *Corros. Sci.*, 2003, **45**(8), 1733–1746.
145 R. K. Gupta, *et al.*, Electrochemical Behavior and Localized Corrosion Associated with Mg2Si Particles in Al and Mg Alloys, *ECS Electrochem. Lett.*, 2012, **1**(1), C1.
146 O. Gharbi and N. Birbilis, Clarifying the Dissolution Mechanisms and Electrochemistry of Mg2Si as a Function of Solution pH, *J. Electrochem. Soc.*, 2018, **165**, C497–C501.
147 F. Eckermann, *et al.*, The influence of MgSi particle reactivity and dissolution processes on corrosion in Al–Mg–Si alloys, *Electrochim. Acta*, 2008, **54**(2), 844–855.
148 F.-l. Zeng, *et al.*, Corrosion mechanism associated with Mg2Si and Si particles in Al–Mg–Si alloys, *Trans. Nonferrous Met. Soc. China*, 2011, **21**(12), 2559–2567.
149 L. L. Li, *et al.*, SVET Study of Galvanic Corrosion of Al/Mg2Si Couple in Aqueous Solutions at Different pH, *J. Electrochem. Soc.*, 2017, **164**(6), C240.
150 J. Wloka, G. Bürklin and S. Virtanen, Influence of second phase particles on initial electrochemical properties of AA7010-T76, *Electrochim. Acta*, 2007, **53**(4), 2055–2059.
151 K. A. Yasakau, *et al.*, Role of intermetallic phases in localized corrosion of AA5083, *Electrochim. Acta*, 2007, **52**(27), 7651–7659.
152 V. Guillaumin, P. Schmutz and G. S. Frankel, Characterization of Corrosion Interfaces by the Scanning Kelvin Probe Force Microscopy Technique, *J. Electrochem. Soc.*, 2001, **148**(5), B163.
153 J. J. Kearns, Aluminum–lithium alloys for aerospace applications: Past, present, and future, *JOM*, 2002, **54**(10), 33–36.
154 A. J. Ardell, Aluminum–lithium alloys, in *ASM Handbook, Volume 2: Properties and Selection of Aluminum Alloys*,ed. M. E. Brown and P. C. S. Haynes, ASM International, 2003, pp. 354–360.
155 J. R. Davis, *Aluminum and Aluminum Alloys*, ASM International, 2001.
156 C. Y. Baik, D. H. Kim, Y. J. Kim and K. R. Lee, Corrosion behavior of Al–3Li alloy in acidic solution, *Mater. Sci. Eng., A*, 2005, **392**(1–2), 163–169.
157 Y. Jiang, C. Zhang, X. Huang, M. Li and Y. Li, Corrosion behavior of Al–3Li alloy in NaCl solution, *J. Mater. Eng. Perform.*, 2015, **24**(11), 4279–4286.
158 X. Zhao, S. Wang and C. Wu, Structural, mechanical and electrochemical properties of Al3Li as anode material for lithium-ion batteries: a first-principles study, *Electrochim. Acta*, 2017, **251**, 308–316.
159 X. Zhao, X. Zhu and G. Chen, Corrosion behavior of Al–Li alloy in NaOH solution containing NaCl, *Rare Met. Mater. Eng.*, 2017, **46**(6), 1549–1554.
160 Z. Wang, C. Dong, Y. Yan, X. Liu and W. Ren, Corrosion inhibition of rare earth element cerium on Al–Li alloy in NaCl solution, *J. Rare Earths*, 2019, **37**(3), 273–280.
161 K. Wang, H. Wang, X. Gao, Q. Wang and J. Shi, The effect of chloride ions on the pitting corrosion behavior of Al3Li alloy in NaCl solution, *Corros. Sci.*, 2016, **109**, 62–69.
162 X. Liu, S. Li, Y. Tang, K. Wang, L. Wang and B. Zhang, Effects of surface treatments on corrosion behaviors of Al3Li alloy in chloride solution, *Mater. Sci. Eng., A*, 2017, **682**, 119–128.
163 Y. Liu, R. Guan, L. Wang and F. Wang, Effects of pH and chloride ion concentration on pitting corrosion behavior of Mg–Zn alloy in NaCl solution, *J. Magnesium Alloys*, 2017, **5**(4), 377–384.
164 K. Wang, H. Wang, X. Gao, Q. Wang and J. Shi, Effect of electropolishing on the pitting corrosion behavior of Al3Li alloy in NaCl solution, *Surf. Coat. Technol.*, 2017, **313**, 51–59.

© 2024 The Author(s). Published by the Royal Society of Chemistry

Open Access Article. Published on 09 October 2024. Downloaded on 7/19/2025 2:17:10 AM.
This article is licensed under a Creative Commons Attribution-NonCommercial 3.0 Unported Licence.

165 K. Wang, Y. Gong, H. Wang, X. Gao and J. Shi, A review of Al3Li as an anode material for lithium-ion batteries, *J. Mater. Sci.*, 2019, **54**(9), 6701–6717.
166 X. Gao, K. Wang, H. Wang, Z. Cao, X. Li and J. Shi, Galvanic corrosion behavior of Al3Li alloy coupled with different metals in NaCl solution, *J. Mater. Sci. Technol.*, 2020, **45**, 85–93.
167 R. Javaherdashti, M. Golestani and H. R. Salimijazi, Investigation of galvanic corrosion of aluminum lithium 8090 alloy with copper alloy C70600 in a 3.5 wt.% NaCl solution, *Corros. Eng., Sci. Technol.*, 2021, **56**(5), 410–415.
168 A. Atrens and M. Liu, Corrosion mechanisms of magnesium alloys, *Adv. Eng. Mater.*, 2001, **3**(9), 689–703.
169 J. Han, Z. Zhang, X. Liu, J. Liu and P. Song, Effect of halide ions on the corrosion behavior of Al–Li alloy, *Rare Met. Mater. Eng.*, 2018, **47**(8), 2276–2281.
170 D. W. Brenner, G. L. Song, A. Atrens, M. S. Dargusch and M. Liu, Corrosion mechanisms of magnesium alloys, *Adv. Eng. Mater.*, 2005, **7**(5), 283–302.
171 G. Song, Y. Li, Y. Li and Y. Du, Effect of Zn content on the electrochemical behavior of Mg–Zn alloys in simulated body fluid, *Mater. Sci. Eng., C*, 2021, **123**, 111979.
172 X. Chen, J. Li, F. Yang and A. Ma, The effect of microstructure on the electrochemical behavior of Mg–Zn alloys, *Mater. Today Commun.*, 2020, **24**, 101146.
173 D. B. Panemangalore, R. Shabadi, M. Gupta and G. Ji, Effect of fluoride coatings on the corrosion behavior of Mg–Zn–Er alloys, *Surf. Interfaces*, 2019, **14**, 72–81.
174 X. Zhang, Y. Li, H. Zhang, M. Wang and C. Feng, Corrosion behavior and mechanism of Mg–Zn alloy in acid and alkaline solutions, *Mater. Res. Express*, 2019, **6**(11), 116512.
175 L. Wu, Y. Gao, Y. Zhu and R. Song, The influence of sulfate ion on the pitting corrosion behavior of Mg–Zn alloy in simulated marine environment, *Corros. Sci.*, 2018, **135**, 66–75.
176 A. I. Ikeuba, B. Zhang, J. Wang, E.-H. Han, W. Ke and P. C. Okafor, SVET and SIET Study of Galvanic Corrosion of Al/$MgZn_2$ in Aqueous Solutions at Different pH, *J. Electrochem. Soc.*, 2018, **165**(3), C180–C194.
177 D. H. Kim, J. G. Kim, H. Y. Kim, H. E. Kim and C. S. Lee, Galvanic corrosion behavior of AZ31B magnesium alloy coupled with copper in 3.5 wt% NaCl solution, *J. Magnesium Alloys*, 2017, **5**(1), 64–70.
178 M. Li, Y. Zheng, L. Zhou, E. Han and W. Ke, Corrosion behavior of Mg–Zn alloy in chloride solution: effect of pH value and Cl-concentration, *J. Alloys Compd.*, 2018, **743**, 218–226.
179 C. Guo, Y. Yu, Y. Cheng and X. Zhang, Corrosion behavior and mechanism of Mg–Zn alloy in simulated seawater with and without Cl-ions, *J. Mater. Sci. Technol.*, 2019, **35**(2), 248–256.
180 B. O. Okonkwo, H. Ming, Z. Zhang, J. Wang, E. Rahimi, S. Hosseinpour and A. Davoodi, Microscale investigation of the correlation between microstructure and galvanic corrosion of low alloy steel A508 and its welded 309/308L stainless steel overlayer, *Corros. Sci.*, 2019, **154**, 49.
181 B. O. Okonkwo, H. Ming, J. Wang, E.-H. Han, E. Rahimi, A. Davoodi and S. Hosseinpour, A new method to determine the synergistic effects of area ratio and microstructure on the galvanic corrosion of LAS 508/309L/308L SS dissimilar metals weld, *J. Mater. Sci. Technol.*, 2021, **78**, 38–50.
182 Z. Jia, L. Liu, Y. He and Y. Wang, Formation and corrosion resistance of surface films on Mg–Zn–Ca alloy in simulated body fluid, *J. Mater. Sci. Technol.*, 2019, **35**(6), 1016–1024.
183 A. I. Ikeuba and B. Zhang, Electrochemical investigation of the anodic hydrogen evolution on MgZn2, Mg2Si, and Al4Cu2Mg8Si7 intermetallic phases, *J. Solid State Electrochem.*, 2023, **27**(1), 111–123.